

Fused RSOS Lattice Models as Higher-Level Nonunitary Minimal Cosets

Elena Tartaglia and Paul A. Pearce

*School of Mathematics and Statistics, University of Melbourne
Parkville, Victoria 3010, Australia*

elena.tartaglia@unimelb.edu.au

p.pearce@ms.unimelb.edu.au

Abstract

We consider the Forrester-Baxter RSOS lattice models with crossing parameter $\lambda = (m' - m)\pi/m'$ in Regime III. In the continuum scaling limit, these models are described by the minimal models $\mathcal{M}(m, m')$. We conjecture that, for $\lambda < \pi/n$, the $n \times n$ fused RSOS models with $n \geq 2$ are described by the higher-level coset $(A_1^{(1)})_k \otimes (A_1^{(1)})_n / (A_1^{(1)})_{k+n}$ at fractional level $k = nM / (M' - M) - 2$ with $(M, M') = (nm - (n-1)m', m')$. To support this conjecture, we investigate the one-dimensional sums arising from Baxter's off-critical corner transfer matrices. In unitary cases ($m = m' - 1$) it is known that, up to leading powers of q , these coincide with the branching functions $b_{r,s,\ell}^{m'-n, m', n}(q)$. For general nonunitary cases ($m < m' - 1$), we identify the ground state one-dimensional RSOS paths and relate them to the quantum numbers (r, s, ℓ) in the various sectors. For $n = 1, 2, 3$, we obtain the local energy functions $H(a, b, c)$ in a suitable gauge and verify that the associated one-dimensional sums produce finitized forms that converge, as N becomes large, to the fractional level branching functions $b_{r,s,\ell}^{M, M', n}(q)$. Extending the work of Schilling, we also conjecture finitized bosonic branching functions $b_{r,s,\ell}^{M, M', n; (N)}(q)$ for general n and check that these agree with the one-dimensional sums for $n = 1, 2, 3$ out to system sizes $N = 14$. Lastly, the finitized Kac characters $\chi_{r,s,\ell}^{P, P', n; (N)}(q)$ of the $n \times n$ fused logarithmic minimal models $\mathcal{LM}(p, p')$ are obtained by taking the *logarithmic limit* $m, m' \rightarrow \infty$ with $m'/m \rightarrow p'/p+$.

arXiv:1509.07576v2 [hep-th] 2 Apr 2017

Contents

1	Introduction	3
2	Higher-Level Nonunitary Minimal Cosets $\mathcal{M}(M, M', n)$	4
2.1	Coset construction and central charges	4
2.2	Branching functions	5
2.3	Conformal weights and Kac tables	6
3	One-Dimensional Sums of Fused RSOS(m, m') Lattice Models	7
3.1	Forrester-Baxter RSOS(m, m') lattice models	7
3.2	Fused RSOS(m, m') lattice models	8
3.2.1	Construction of $n \times n$ fused face weights	8
3.2.2	Local properties of $n \times n$ fused face weights	9
3.3	Fused RSOS paths, shaded bands and ground states	9
3.3.1	Paths, shaded band diagrams and sectors	9
3.3.2	Fused RSOS ground state boundary conditions	10
3.4	Local energies and one-dimensional sums	11
3.4.1	Local energy functions	11
3.4.2	Energy statistic and one-dimensional sums	13
3.4.3	$n = 1$ local energies	14
3.4.4	$n = 2$ local energies	16
3.4.5	$n = 3$ local energies	16
4	Conjectured Finitized Bosonic Branching Functions	18
4.1	Finitized bosonic branching functions	18
4.2	Logarithmic limit and finitized Kac characters	20
5	Conclusion	21
A	Elliptic Functions	21
B	Counting of Contiguous Shaded Bands	22
B.1	Counting of shaded n -bands	22
B.2	Proof that $\rho = r \bmod n$	24
C	$n = 2, 3$ Face Weights	24
C.1	Explicit 2×2 fused face weights	24
C.2	Explicit 3×3 fused face weights	25
D	$n = 2, 3$ Diagonal Conjugate Modulus Face Weights	26
D.1	Explicit 2×2 conjugate modulus face weights	26
D.2	Explicit 3×3 conjugate modulus face weights	27

1 Introduction

Solid-On-Solid (SOS) models with unbounded heights and Restricted Solid-On-Solid (RSOS) models with bounded heights were originally used [1–4] to study fluctuating surfaces and the roughening transition. The SOS condition ensures columns of solid with no overhangs. The $A_{m'-1}$ RSOS(m, m') models of Andrews, Baxter and Forrester [5, 6] in Regime III, with heights $1 \leq a \leq m' - 1$, are exactly solvable RSOS models in the sense that they are Yang-Baxter integrable [7]. The RSOS(m, m') models have crossing parameter $\lambda = (m' - m)\pi/m'$ with $2 \leq m < m'$ and $\gcd(m, m') = 1$. The RSOS(3, 4) model is the Ising model and the RSOS($m' - 1, m'$) models with $m' \geq 4$ realize [8] the \mathbb{Z}_2 universality classes of multicritical Ising models. The universal behaviour of such systems is described in the continuum by Conformal Field Theories (CFTs) [9]. Indeed it is now well established that, in the continuum scaling limit, the RSOS(m, m') models in Regime III realize the unitary [10] ($m = m' - 1$) and nonunitary [11–14] ($m < m' - 1$) minimal models $\mathcal{M}(m, m')$ of Belavin, Polyakov and Zamolodchikov [15]. In fact, the minimal models $\mathcal{M}(m, m')$ represent the simplest family of rational coset CFTs [16, 17].

On the one hand, lattice fusion [18–21] of $n \times n$ blocks of elementary face weights of the RSOS(m, m') models yields the fused Yang-Baxter integrable lattice models RSOS(m, m') $_{n \times n}$. On the other hand, higher fusion level minimal models $\mathcal{M}(M, M', n)$ at integer fusion level $n \geq 1$ and fractional level $k = nM/(M' - M) - 2$ can be constructed [22–27] as the Goddard-Kent-Olive (GKO) cosets $(A_1^{(1)})_k \otimes (A_1^{(1)})_n / (A_1^{(1)})_{k+n}$ (2.6). For $n = 1$, these are the minimal models [15, 16] $\mathcal{M}(m, m') = \mathcal{M}(M, M', 1)$ with $(M, M') = (m, m')$. For $n = 2$, these are the superconformal minimal models [17] $\mathcal{M}(M, M', 2)$. For unitary cases ($m = m' - 1$) the known identification [19–21, 28–30], in the continuum scaling limit, is given by $(M, M') = (m' - n, m')$. In particular, the one-dimensional sums arising from Baxter’s Corner Transfer Matrices (CTMs) [31] coincide, up to leading powers of q , with the coset branching functions $b_{r,s,\ell}^{M'-n, M', n}(q)$ [22]. This observation is in agreement with the *correspondence principle* of the Kyoto school [32] which is generally valid in Regime III.

The consequences of the identification of the unitary RSOS($m' - 1, m'$) $_{n \times n}$ model with the coset CFT $\mathcal{M}(m' - n, m', n)$ are twofold. First the conformal data, and therefore the universality class and all of the universal critical exponents, are exactly determined for these RSOS(m, m') lattice models. Second, the integrable lattice regularizations can be used [33] to study further properties of these coset CFTs and their integrable off-critical $\varphi_{1,3}$ thermal perturbations.

In this paper, we generalize the identification of $n \times n$ fused RSOS(m, m') lattice models with coset CFTs to the nonunitary cases. Specifically we conjecture that, for $\lambda < \pi/n$, the general nonunitary $n \times n$ fused RSOS(m, m') lattice models with $m < m' - 1$ are described, in the continuum scaling limit, by the higher-level coset $(A_1^{(1)})_k \otimes (A_1^{(1)})_n / (A_1^{(1)})_{k+n}$ at fractional level $k = nM/(M' - M) - 2$ with $(M, M') = (nm - (n-1)m', m')$

$$\text{RSOS}(m, m')_{n \times n} \simeq \mathcal{M}(M, M', n), \quad (M, M') = (nm - (n-1)m', m') \quad (1.1)$$

To support this conjecture, we investigate the one-dimensional sums arising from Baxter’s off-critical CTMs. We identify the ground state one-dimensional RSOS paths and relate them to the quantum numbers (r, s, ℓ) in the various sectors. For $n = 1, 2, 3$, we obtain local energy functions $H(\sigma_{j-1}, \sigma_j, \sigma_{j+1})$ in a suitable gauge and, using Mathematica [34], we verify that the one-dimensional sums produce finitized fermionic forms which, for large N , converge to the fractional level branching functions $b_{r,s,\ell}^{M, M', n}(q)$. Lastly, extending the results of Schilling [30], we conjecture finitized bosonic branching functions $b_{r,s,\ell}^{M, M', n; (N)}(q)$ for general n using q -multinomials [30, 35] and check that these agree with the one-dimensional sums for $n = 1, 2, 3$.

There are a number mathematical and physical motivations for studying nonunitary RSOS models arising from different areas of application. Although nonunitary RSOS models in two dimensions have some negative Boltzmann face weights and lack a strict probabilistic interpretation, the associated CFTs

and 1-dimensional quantum Hamiltonians are well defined and physical. Indeed, the form of the critical Hamiltonians in Regime III was recently generalized to off-critical Hamiltonians in [36]. In statistical mechanics, the Lee-Yang $\mathcal{M}(2, 5)$ theory [37] describes [38–40] the closing, in the complex magnetic field plane, of the gap in the distribution of Lee-Yang zeros of the two-dimensional ferromagnetic Ising model $\mathcal{M}(3, 4)$. In Quantum Field Theory (QFT), $\mathcal{M}(2, 5)$ [41, 42] and $\mathcal{M}(3, 5)$ [43] describe simple one-particle massive scattering theories. More general theories describe scattering theories with kinks and breathers. The RSOS(m, m') models provide lattice regularizations of these field theories. In the context of anyons and the Fractional Quantum Hall Effect (FQHE), $\mathcal{M}(3, 5)$ [44] has been used to describe spinless electrons at filling fraction $\nu = 2/5$. In condensed matter physics, nonunitary RSOS models have also been studied recently to shed light on the properties of quantum entanglement [45]. It is therefore generally important to understand the physical consequences of the loss of unitarity. This is particularly relevant in the study of statistical systems with nonlocal degrees of freedom which are described by logarithmic CFTs [46, 47] and are invariably nonunitary. Such theories, exemplified by the logarithmic minimal models $\mathcal{LM}(p, p')$ [48] and their fused counterparts [49, 50], can be studied by taking the logarithmic limit [51] of rational nonunitary minimal models as in Section 4.2. These exactly solvable families contain many generalized lattice models of critical polymers and critical percolation in two dimensions. Perhaps most importantly, from a mathematical perspective, the fusion hierarchies RSOS(m, m') $_{n \times n'}$ encode [29] the integrability of these nonunitary minimal models through their T - and Y -systems.

The layout of the paper is as follows. In Section 2, we describe cosets with integer fusion level n and fractional level k and present explicit formulas for their central charges, conformal weights and branching functions. In Section 3, we use techniques coming from CTMs to set up the associated one-dimensional sums of the $n \times n$ fused RSOS(m, m') lattice models in Regime III. For $n = 1, 2, 3$, we explicitly calculate the local energies. In Section 4, generalizing the results of Schilling [30] to nonunitary cases, we present a conjecture for the finitized bosonic branching functions for general n . For $n = 1, 2, 3$ and out to order $N = 14$, we verify that (up to the leading terms involving the central charges and conformal dimensions) the one-dimensional sums agree with the bosonic forms and give finitized forms of the fractional level branching functions $b_{r,s,\ell}^{M,M',n}(q)$. In Appendix A, we collect relevant properties of elliptic functions. In Appendix B, we establish the counting and properties of contiguous shaded or unshaded bands. In Appendix C, we list the explicit fused RSOS face weights for $n = 2$ and $n = 3$. In Appendix D, we list the explicit conjugate modulus forms of the diagonal fused face weights for $n = 2$ and $n = 3$. We finish with some concluding remarks.

2 Higher-Level Nonunitary Minimal Cosets $\mathcal{M}(M, M', n)$

2.1 Coset construction and central charges

The minimal models $\mathcal{M}(m, m')$ [15], with coprime integers m, m' satisfying $2 \leq m < m'$, are rational Conformal Field Theories (CFTs) with central charges

$$c = 1 - \frac{6(m - m')^2}{mm'}, \quad 2 \leq m < m', \quad \gcd(m, m') = 1 \quad (2.1)$$

The conformal weights and associated Virasoro characters are

$$\Delta_{r,s}^{m,m'} = \frac{(rm' - sm)^2 - (m - m')^2}{4mm'}, \quad 1 \leq r \leq m - 1, \quad 1 \leq s \leq m' - 1 \quad (2.2)$$

$$\text{ch}_{r,s}^{m,m'}(q) = \frac{q^{-c/24 + \Delta_{r,s}^{m,m'}}}{(q)_\infty} \sum_{k=-\infty}^{\infty} [q^{k(kmm' + rm' - sm)} - q^{(km+r)(km'+s)}] \quad (2.3)$$

where the q -factorials are

$$(q)_n = \prod_{k=1}^n (1 - q^k), \quad (q)_\infty = \prod_{k=1}^{\infty} (1 - q^k) \quad (2.4)$$

In these expressions, $q = e^{\pi i \tau}$ is the modular nome.

Algebraically, the higher-level minimal models are constructed [26, 27] as cosets

$$\mathcal{M}(M, M', n) \simeq \text{COSET}\left(\frac{nM}{M'-M} - 2, n\right), \quad \text{gcd}\left(\frac{M'-M}{n}, M'\right) = 1, \quad 2 \leq M < M', \quad n, M, M' \in \mathbb{N} \quad (2.5)$$

where $n = 1, 2, \dots$ is the integer fusion level, $k = \frac{nM}{M'-M} - 2$ is the fractional fusion level and \mathbb{N} denotes the set of positive integers. The diagonal GKO coset [16, 17] takes the form

$$\text{COSET}(k, n) : \quad \frac{(A_1^{(1)})_k \oplus (A_1^{(1)})_n}{(A_1^{(1)})_{k+n}}, \quad k = \frac{\hat{p}}{\hat{p}'} - 2, \quad \text{gcd}(\hat{p}, \hat{p}') = 1, \quad n, \hat{p}, \hat{p}' \in \mathbb{N} \quad (2.6)$$

where the subscripts on the affine $su(2)$ current algebra $A_1^{(1)}$ denote the respective levels k , n and $k+n$. The central charge of the coset Virasoro algebra is thus given by

$$c = c_k + c_n - c_{k+n} = \frac{3kn(k+n+4)}{(k+2)(n+2)(k+n+2)} \quad (2.7)$$

where the central charge of the affine current algebra $(A_1^{(1)})_k$ is

$$c_k = \frac{3k}{k+2} \quad (2.8)$$

The central charges of the minimal models $\mathcal{M}(M, M', n)$ are thus

$$c^{M, M', n} = \frac{3n}{n+2} \left[1 - \frac{2(n+2)(M'-M)^2}{n^2 M M'} \right], \quad 2 \leq M < M', \quad \text{gcd}\left(\frac{M'-M}{n}, M'\right) = 1 \quad (2.9)$$

The usual minimal models [15] are given by $n = 1$. The superconformal minimal models are given by the specialization $n = 2$ with central charges

$$c^{M, M', 2} = \frac{3}{2} \left[1 - \frac{2(M'-M)^2}{M M'} \right], \quad 2 \leq M < M', \quad \text{gcd}\left(\frac{M'-M}{2}, M'\right) = 1 \quad (2.10)$$

2.2 Branching functions

The characters of the higher fusion level minimal models $\mathcal{M}(M, M', n)$ are given by the branching functions $b_{r,s,\ell}^{M, M', n}(q)$ [26, 27] of the coset (2.5). These are expressible in terms of the string functions [22, 52–55] of \mathbb{Z}_n parafermions with central charge $c = \frac{2n-2}{n+2}$. For the fundamental domain

$$0 \leq m \leq \ell \leq n, \quad \ell - m \in 2\mathbb{Z}, \quad m, \ell = 0, 1, \dots, n, \quad n \in \mathbb{N} \quad (2.11)$$

the string functions are given by

$$\begin{aligned} c_m^\ell(q) &= \frac{q^{-\frac{1}{24} \frac{2n-2}{n+2} + \frac{\ell(\ell+2)}{4(n+2)} - \frac{m^2}{4n}}}{(q)_\infty^3} \sum_{i,j=0}^{\infty} (-1)^{i+j} q^{ij(n+1) + \frac{1}{2}i(i+1) + \frac{1}{2}j(j+1)} \\ &\quad \times \left[q^{\frac{i}{2}(\ell+m) + \frac{j}{2}(\ell-m)} - q^{n-\ell+1 + \frac{i}{2}(2n+2-\ell-m) + \frac{j}{2}(2n+2-\ell+m)} \right] \end{aligned} \quad (2.12)$$

where the dependence on n has been suppressed. The \mathbb{Z}_n parafermionic index m should not be confused with the minimal model label m in (m, m', n) . The fundamental domain of definition (2.11) of the string functions is extended to the domain

$$\ell = 0, 1, \dots, n, \quad m \in \mathbb{Z}, \quad n \in \mathbb{N} \quad (2.13)$$

by setting $c_m^\ell(q) = 0$ for $\ell - m \notin 2\mathbb{Z}$ and using the symmetries

$$c_m^\ell(q) = c_{-m}^\ell(q) = c_{n-m}^{n-\ell}(q) = c_{m+2n}^\ell(q) \quad (2.14)$$

so that $c_m^\ell(q)$ is even and periodic in m with period $2n$.

Explicitly, on the checkerboard $r + s = \ell \pmod{2}$, the branching functions are given by

$$b_{r,s,\ell}^{M,M',n}(q) = q^{\Delta_{r,s}^{M,M',n} - \frac{c^{M,M',n}}{24} + \frac{n-1}{12(n+2)}} \times \sum_{\substack{0 \leq m \leq n/2 \\ m = \ell/2 \pmod{1}}} c_{2m}^\ell(q) \left[\sum_{\substack{j \in \mathbb{Z} \\ m_{r-s}(j) = \pm m \pmod{n}}} q^{\frac{j}{n}(jMM' + rM' - sM)} - \sum_{\substack{j \in \mathbb{Z} \\ m_{r+s}(j) = \pm m \pmod{n}}} q^{\frac{j}{n}(jM' + s)(jM + r)} \right], \quad (2.15)$$

$$1 \leq r \leq M - 1, \quad 1 \leq s \leq M' - 1, \quad \ell = 0, 1, \dots, n$$

where the first sum (on m) runs over integers (ℓ even) or half odd integers (ℓ odd) with

$$m_a(j) := a/2 + jM' \quad (2.16)$$

The cosets are quotients of the algebra $(A_1^{(1)})_k \oplus (A_1^{(1)})_n$ by the subalgebra $(A_1^{(1)})_{k+n}$. It follows that products of the characters of the algebras $(A_1^{(1)})_k$ and $(A_1^{(1)})_n$ decompose as linear sums of the characters of $(A_1^{(1)})_{k+n}$. The coefficients are branching functions which play the role of the multiplicities in the restriction of classical groups. These branching functions satisfy the decomposition or *branching rules* [22, 26, 27]

$$\widehat{\text{ch}}_{r,s}^{\hat{p},\hat{p}'}(q, z) \widehat{\text{ch}}_{r',0}^{n+2,1}(q, z) = \sum_{\substack{\sigma=1 \\ \sigma = r+\ell \pmod{2}}}^{\hat{p}+n\hat{p}'-1} b_{r,\sigma,\ell}^{\hat{p},\hat{p}+n\hat{p}',n}(q) \widehat{\text{ch}}_{\sigma,s}^{\hat{p}+n\hat{p}',\hat{p}'}(q, z), \quad \hat{p} = M, \quad \hat{p}' = \frac{M'-M}{n} \quad (2.17)$$

relating admissible characters $\widehat{\text{ch}}_{r,s}^{\hat{p},\hat{p}'}$ of affine current algebras $(A_1^{(1)})_k$, $(A_1^{(1)})_n$, $(A_1^{(1)})_{k+n}$ with

$$r' = \begin{cases} n+1-\ell, & s \text{ odd} \\ \ell+1, & s \text{ even} \end{cases} \quad \ell = 0, 1, \dots, n \quad (2.18)$$

For $n = 1$ and $n = 2$, the branching functions reduce to the Virasoro minimal and superconformal characters respectively.

2.3 Conformal weights and Kac tables

Explicitly, for $r + s = \ell \pmod{2}$, the $\mathcal{M}(M, M', n)$ conformal weights are [49]

$$\Delta_{r,s,\ell}^{M,M',n} = \Delta_{r,s}^{M,M',n} + \Delta_{r-s}^{\ell,n} + \text{Max}[\frac{1}{2}(\ell+2-r-s), 0] + \text{Max}[\frac{1}{2}(\ell'+2-(M-r)-(M'-s)), 0] \quad (2.19)$$

The first term on the right and ℓ' are given by

$$\Delta_{r,s}^{M,M',n} = \frac{(rM' - sM)^2 - (M' - M)^2}{4nMM'}, \quad \ell' = \begin{cases} \ell, & \frac{M'-M}{n} \text{ even} \\ n - \ell, & \frac{M'-M}{n} \text{ odd} \end{cases} \quad (2.20)$$

Setting $\bar{m} = m \bmod 2n$, the second term is the conformal weight of the string function $c_m^\ell(q)$

$$\Delta_m^{\ell,n} = \text{Max}[\Delta(\bar{m}, \ell, n), \Delta(2n - \bar{m}, \ell, n), \Delta(n - \bar{m}, n - \ell, n)], \quad \Delta(m, \ell, n) = \frac{\ell(\ell + 2)}{4(n + 2)} - \frac{m^2}{4n} \quad (2.21)$$

folded into the fundamental domain (2.11). The third term only gives a nonzero contribution for $r + s \leq \ell \leq n$. The fourth term is the counterpart of the third term under the Kac table symmetry. It only contributes for $r + s \geq M + M' - \ell \geq M + M' - n$. The conformal weights are thus conveniently organized into $n + 1$ layered Kac tables each displaying the checkerboard pattern and satisfying the Kac table symmetry

$$\Delta_{r,s,\ell}^{M,M',n} = \begin{cases} \Delta_{M-r, M'-s, \ell}^{M, M', n} & \frac{M'-M}{n} \text{ even} \\ \Delta_{M-r, M'-s, n-\ell}^{M, M', n} & \frac{M'-M}{n} \text{ odd} \end{cases} \quad (2.22)$$

The Kac tables of $\mathcal{M}(3, 7, 2)$ and $\mathcal{M}(5, 7, 2)$ are shown in Table 1.

s															
6	<table border="1" style="border-collapse: collapse; text-align: center;"><tr><td style="background-color: #e6e6fa;">$\frac{11}{16}$</td><td>$0, \frac{3}{2}$</td></tr><tr><td>$\frac{2}{7}, \frac{11}{14}$</td><td style="background-color: #e6e6fa;">$-\frac{3}{112}$</td></tr><tr><td style="background-color: #e6e6fa;">$\frac{13}{112}$</td><td>$\frac{3}{7}, -\frac{1}{14}$</td></tr><tr><td>$\frac{3}{7}, -\frac{1}{14}$</td><td style="background-color: #e6e6fa;">$\frac{13}{112}$</td></tr><tr><td style="background-color: #e6e6fa;">$-\frac{3}{112}$</td><td>$\frac{2}{7}, \frac{11}{14}$</td></tr><tr><td>1</td><td><table border="1" style="border-collapse: collapse; text-align: center;"><tr><td>$0, \frac{3}{2}$</td><td style="background-color: #e6e6fa;">$\frac{11}{16}$</td></tr></table></td></tr> </table>	$\frac{11}{16}$	$0, \frac{3}{2}$	$\frac{2}{7}, \frac{11}{14}$	$-\frac{3}{112}$	$\frac{13}{112}$	$\frac{3}{7}, -\frac{1}{14}$	$\frac{3}{7}, -\frac{1}{14}$	$\frac{13}{112}$	$-\frac{3}{112}$	$\frac{2}{7}, \frac{11}{14}$	1	<table border="1" style="border-collapse: collapse; text-align: center;"><tr><td>$0, \frac{3}{2}$</td><td style="background-color: #e6e6fa;">$\frac{11}{16}$</td></tr></table>	$0, \frac{3}{2}$	$\frac{11}{16}$
$\frac{11}{16}$	$0, \frac{3}{2}$														
$\frac{2}{7}, \frac{11}{14}$	$-\frac{3}{112}$														
$\frac{13}{112}$	$\frac{3}{7}, -\frac{1}{14}$														
$\frac{3}{7}, -\frac{1}{14}$	$\frac{13}{112}$														
$-\frac{3}{112}$	$\frac{2}{7}, \frac{11}{14}$														
1	<table border="1" style="border-collapse: collapse; text-align: center;"><tr><td>$0, \frac{3}{2}$</td><td style="background-color: #e6e6fa;">$\frac{11}{16}$</td></tr></table>	$0, \frac{3}{2}$	$\frac{11}{16}$												
$0, \frac{3}{2}$	$\frac{11}{16}$														
1	1 2 r														

s																														
6	<table border="1" style="border-collapse: collapse; text-align: center;"><tr><td style="background-color: #e6e6fa;">$\frac{31}{16}$</td><td>$\frac{9}{10}, \frac{7}{5}$</td><td style="background-color: #e6e6fa;">$\frac{27}{80}$</td><td>$\frac{3}{2}, 0$</td></tr><tr><td>5</td><td>$\frac{8}{7}, \frac{23}{14}$</td><td style="background-color: #e6e6fa;">$\frac{269}{560}$</td><td>$\frac{19}{35}, \frac{3}{70}$</td><td style="background-color: #e6e6fa;">$\frac{9}{112}$</td></tr><tr><td>4</td><td style="background-color: #e6e6fa;">$\frac{73}{112}$</td><td>$\frac{43}{70}, \frac{4}{35}$</td><td style="background-color: #e6e6fa;">$\frac{29}{560}$</td><td>$\frac{3}{14}, \frac{5}{7}$</td></tr><tr><td>3</td><td>$\frac{5}{7}, \frac{3}{14}$</td><td style="background-color: #e6e6fa;">$\frac{29}{560}$</td><td>$\frac{4}{35}, \frac{43}{70}$</td><td style="background-color: #e6e6fa;">$\frac{73}{112}$</td></tr><tr><td>2</td><td style="background-color: #e6e6fa;">$\frac{9}{112}$</td><td>$\frac{3}{70}, \frac{19}{35}$</td><td style="background-color: #e6e6fa;">$\frac{269}{560}$</td><td>$\frac{23}{14}, \frac{8}{7}$</td></tr><tr><td>1</td><td>$0, \frac{3}{2}$</td><td style="background-color: #e6e6fa;">$\frac{27}{80}$</td><td>$\frac{7}{5}, \frac{9}{10}$</td><td style="background-color: #e6e6fa;">$\frac{31}{16}$</td></tr> </table>	$\frac{31}{16}$	$\frac{9}{10}, \frac{7}{5}$	$\frac{27}{80}$	$\frac{3}{2}, 0$	5	$\frac{8}{7}, \frac{23}{14}$	$\frac{269}{560}$	$\frac{19}{35}, \frac{3}{70}$	$\frac{9}{112}$	4	$\frac{73}{112}$	$\frac{43}{70}, \frac{4}{35}$	$\frac{29}{560}$	$\frac{3}{14}, \frac{5}{7}$	3	$\frac{5}{7}, \frac{3}{14}$	$\frac{29}{560}$	$\frac{4}{35}, \frac{43}{70}$	$\frac{73}{112}$	2	$\frac{9}{112}$	$\frac{3}{70}, \frac{19}{35}$	$\frac{269}{560}$	$\frac{23}{14}, \frac{8}{7}$	1	$0, \frac{3}{2}$	$\frac{27}{80}$	$\frac{7}{5}, \frac{9}{10}$	$\frac{31}{16}$
$\frac{31}{16}$	$\frac{9}{10}, \frac{7}{5}$	$\frac{27}{80}$	$\frac{3}{2}, 0$																											
5	$\frac{8}{7}, \frac{23}{14}$	$\frac{269}{560}$	$\frac{19}{35}, \frac{3}{70}$	$\frac{9}{112}$																										
4	$\frac{73}{112}$	$\frac{43}{70}, \frac{4}{35}$	$\frac{29}{560}$	$\frac{3}{14}, \frac{5}{7}$																										
3	$\frac{5}{7}, \frac{3}{14}$	$\frac{29}{560}$	$\frac{4}{35}, \frac{43}{70}$	$\frac{73}{112}$																										
2	$\frac{9}{112}$	$\frac{3}{70}, \frac{19}{35}$	$\frac{269}{560}$	$\frac{23}{14}, \frac{8}{7}$																										
1	$0, \frac{3}{2}$	$\frac{27}{80}$	$\frac{7}{5}, \frac{9}{10}$	$\frac{31}{16}$																										
1	1 2 3 4 r																													

	= NS,		= R
--	-------	--	-----

Table 1: Kac tables of conformal weights (2.19) for the superconformal minimal models $\mathcal{M}(3, 7, 2)$ and $\mathcal{M}(5, 7, 2)$ with central charges $c = -\frac{11}{14}, \frac{81}{70}$ respectively. The Neveu-Schwarz (NS) sectors (not shaded) with $r + s$ even correspond to $\ell = 0, 2$ and are shown as the pair $\Delta_{r,s,0}^{M,M',2}, \Delta_{r,s,2}^{M,M',2}$. The conformal weights in these two sectors differ by half-odd integers. The Ramond (R) sectors (shaded) with $r + s$ odd correspond to $\ell = 1$.

3 One-Dimensional Sums of Fused RSOS(m, m') Lattice Models

3.1 Forrester-Baxter RSOS(m, m') lattice models

The Forrester-Baxter RSOS(m, m') lattice models [6], with $2 \leq m < m'$ and m, m' coprime, are defined on a square lattice with heights $a = 1, 2, \dots, m' - 1$ restricted so that nearest neighbour heights differ by ± 1 . The heights thus live on the $A_{m'-1}$ Dynkin diagram. The nonzero Boltzmann face weights in Regime III are

$$W \left(\begin{array}{c|c} a \pm 1 & a \\ a & a \mp 1 \end{array} \middle| u \right) = \begin{array}{c} a \pm 1 \\ \square \\ a \end{array} \begin{array}{c} a \\ u \\ a \mp 1 \end{array} = s(\lambda - u) \quad (3.1)$$

$$W \left(\begin{array}{c|c} a & a \pm 1 \\ a \mp 1 & a \end{array} \middle| u \right) = \begin{array}{c} a \\ \square \\ a \mp 1 \end{array} \begin{array}{c} a \pm 1 \\ u \\ a \end{array} = -\frac{g_{a \pm 1}}{g_{a \mp 1}} \frac{s((a \pm 1)\lambda)}{s(a\lambda)} s(u) \quad (3.2)$$

$$W \left(\begin{array}{c|c} a & a \pm 1 \\ a \pm 1 & a \end{array} \middle| u \right) = \begin{array}{c} a \\ \square \\ a \pm 1 \end{array} \begin{array}{c} a \pm 1 \\ u \\ a \end{array} = \frac{s(a\lambda \pm u)}{s(a\lambda)} \quad (3.3)$$

where $s(u) = \vartheta_1(u, t)/\vartheta_1(\lambda, t)$ is a quotient of the standard elliptic theta functions [56]

$$\vartheta_1(u, t) = 2t^{1/4} \sin u \prod_{n=1}^{\infty} (1 - 2t^{2n} \cos 2u + t^{4n})(1 - t^{2n}), \quad 0 < u < \lambda, \quad 0 < t < 1 \quad (3.4)$$

u is the spectral parameter and g_a are arbitrary gauge factors. Unless stated otherwise, we work in the gauge $g_a = 1$. The elliptic nome $t = e^{-\epsilon}$ is a temperature-like variable, with t^2 measuring the departure from criticality corresponding to the $\varphi_{1,3}$ integrable perturbation [57]. The crossing parameter is

$$\lambda = \frac{(m' - m)\pi}{m'}, \quad 1 \leq m < m', \quad m, m' \text{ coprime} \quad (3.5)$$

where $m \geq 2$ relates to minimal models and $m = 1$ relates to the $\mathbb{Z}_{m'-2}$ parafermions.

3.2 Fused RSOS(m, m') lattice models

3.2.1 Construction of $n \times n$ fused face weights

The RSOS(m, m') $_{n \times n}$ face weights are constructed by fusing $n \times n$ blocks of elementary faces

$$W^{n,n} \left(\begin{array}{c|c} d & c \\ a & b \end{array} \middle| u \right) = \frac{1}{\eta^{n,n}(u)} \begin{array}{c} d \\ \square \\ a \end{array} \begin{array}{c} c \\ u_0 \dots u_{n-2} u_{n-1} \\ b \end{array}, \quad u_j = u + j\lambda \quad (3.6)$$

where the solid dots indicate free sums over the allowed values of the heights. In the gauge $g_a = 1$, the fused weights are independent of the heights at the sites marked with a cross. The fused weights are set to zero unless the adjacent pairs of heights $a, b = 1, \dots, m' - 1$ on each edge satisfy the restrictions

$$|a - b| = \begin{cases} 0, 2, 4, \dots, n, & n \text{ even} \\ 1, 3, 5, \dots, n, & n \text{ odd} \end{cases} \quad n + 2 \leq a + b \leq 2m' - n - 2 \quad (3.7)$$

We therefore see that $\frac{1}{2}(a - b) = -\frac{n}{2}, -\frac{n-1}{2}, \dots, \frac{n-1}{2}, \frac{n}{2}$ is a spin- $\frac{n}{2}$ variable.

The $n \times n$ fused RSOS(m, m') models exhibit a duality under the involution

$$\lambda \leftrightarrow \pi - \lambda \quad \text{or} \quad m \leftrightarrow m' - m \quad (3.8)$$

in the sense that both the spectrum (set of eigenvalues) of the row and corner transfer matrices are invariant. For finite-size systems, the effect of this involution is to turn the eigenvalue spectrum upside down and to interchange the ground states. In particular, the fused RSOS models with $m = m' - 1$, related to the unitary minimal models, are dual to those with $m = 1$ which is not allowed as a minimal model. In fact, unlike the cases $m \geq 2$, the ground states of the fused RSOS models with $m = 1$ possess a $\mathbb{Z}_{m'-2}$ symmetry and relate, in the continuum scaling limit, to $\mathbb{Z}_{m'-2}$ parafermions. In nonunitary cases with $m \geq 2$, this duality maps between RSOS models related to pairs of nonunitary minimal models.

3.2.2 Local properties of $n \times n$ fused face weights

The $n \times n$ fused weights satisfy local relations in the form of the initial condition, the inversion relation and the Yang-Baxter equation

$$\begin{aligned} W^{n,n} \left(\begin{array}{c|c} d & c \\ a & b \end{array} \middle| 0 \right) &= \delta(a, c) \\ \sum_g W^{n,n} \left(\begin{array}{c|c} d & g \\ a & b \end{array} \middle| u \right) W^{n,n} \left(\begin{array}{c|c} d & c \\ g & b \end{array} \middle| -u \right) &= \delta(a, c) \prod_{k=1}^n \frac{s(k\lambda - u)s(k\lambda + u)}{s(k\lambda)^2} \\ \sum_g W^{n,n} \left(\begin{array}{c|c} f & g \\ a & b \end{array} \middle| u \right) W^{n,n} \left(\begin{array}{c|c} e & d \\ f & g \end{array} \middle| u+v \right) W^{n,n} \left(\begin{array}{c|c} d & c \\ g & b \end{array} \middle| v \right) &= \sum_g W^{n,n} \left(\begin{array}{c|c} e & g \\ f & a \end{array} \middle| v \right) W^{n,n} \left(\begin{array}{c|c} g & c \\ a & b \end{array} \middle| u+v \right) W^{n,n} \left(\begin{array}{c|c} e & d \\ g & c \end{array} \middle| u \right) \end{aligned} \quad (3.9)$$

A number of identities in elliptic theta functions are needed to verify these relations. These all follow from the fundamental identity listed in Appendix A. Together, these local relations imply commuting row and corner transfer matrices and exact integrability. The weights are also symmetric under reflection about the leading diagonal and under height reversal

$$W^{n,n} \left(\begin{array}{c|c} d & c \\ a & b \end{array} \middle| u \right) = W^{n,n} \left(\begin{array}{c|c} b & c \\ a & d \end{array} \middle| u \right), \quad W^{n,n} \left(\begin{array}{c|c} d & c \\ a & b \end{array} \middle| u \right) = W^{n,n} \left(\begin{array}{c|c} m'-d & m'-c \\ m'-a & m'-b \end{array} \middle| u \right) \quad (3.10)$$

3.3 Fused RSOS paths, shaded bands and ground states

In this section, we recall the shaded band diagrams of [14] and posit the ground states of the $n \times n$ fused RSOS models. The considerations in this section and the next section on one-dimensional sums are purely combinatorial.

3.3.1 Paths, shaded band diagrams and sectors

A path $\sigma = \{\sigma_0, \sigma_1, \dots, \sigma_N, \sigma_{N+1}\}$ of the $n \times n$ fused RSOS lattice models is an $(N+1)$ -step walk, with $\sigma_j \in A_{m'-1}$, on the level n fused adjacency diagram given by the adjacency rules (3.7). In this paper, we always take N to be even. If n is even, all of the heights σ_j have the same parity (all even or all odd). If n is odd, the heights σ_j alternate in parity along the path. The $(N+1)$ -step RSOS paths are separated into various sectors labelled by the boundary conditions

$$(\sigma_0, \sigma_N, \sigma_{N+1}) = (a, b, c) \quad (3.11)$$

In the continuum scaling limit, the heights (a, b, c) are related to the quantum numbers (r, s, ℓ) . A typical path is shown in Figure 1. Combinatorially, it is convenient to describe these paths as walks on the $A_{m'-1}$ shaded band diagram [14]. The band $(a, a+1)$ between heights a and $a+1$ is shaded if

$$a = \left\lfloor \frac{rm'}{m} \right\rfloor, \quad r = 1, \dots, m-1 \quad (3.12)$$

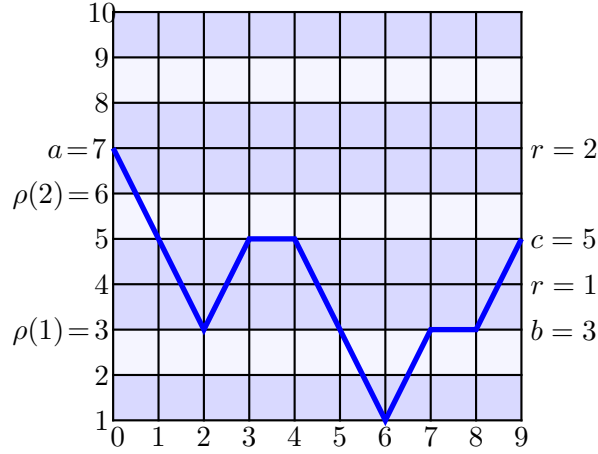


Figure 1: Band diagram showing a typical path $\sigma = \{7, 5, 3, 5, 5, 3, 1, 3, 3, 5\}$ in the sector $(\sigma_0, \sigma_N, \sigma_{N+1}) = (7, 3, 5)$ for the superconformal minimal model $\mathcal{M}(3, 11, 2)$ with $(m, m', n) = (7, 11, 2)$ and $N = 8$. Shaded 1-bands occur at heights $a = 1, 3, 4, 6, 7, 9$ and shaded 2-bands occur at $\rho = \rho(r) = 3, 6$. Since $M - 1 = 2$, the two shaded 2-bands are labelled by $r = 1, 2$. We always take N to be even.

and is otherwise unshaded. Shaded and unshaded bands are interchanged under duality $m \leftrightarrow m' - m$. An n -band consists of n contiguous bands, where each band is shaded or unshaded. If all the 1-bands in an n -band are shaded, we call it a *shaded n -band*. If all the 1-bands in an n -band are unshaded, we call it an *unshaded n -band*. Otherwise, it a *mixed n -band*.

For fixed (m, m', n) , the heights of the shaded n -bands ($\rho, \rho+n$) are labelled by the sequences

$$\rho = \rho(r) = \rho^{m, m', n}(r), \quad r = 1, 2, \dots, M-1 \quad (3.13)$$

Since these are monotonically increasing sequences the inverse exists

$$r = r(\rho) = r^{m, m', n}(\rho), \quad \rho = \rho(1), \rho(2), \dots, \rho(M-1) \quad (3.14)$$

Here $M = M(m, m', n)$ counts the length of the finite sequence. For $n = 1$, $\rho = \rho(r)$ is given by the sequence (3.12). Although these finite sequences are easily enumerated diagrammatically, as in Figure 1, we have been unable to find explicit expressions for these sequences for $n > 1$. Nevertheless in Appendix B we show that, for $0 < \lambda < \pi/n$, the number of shaded n -bands is

$$\# \text{ shaded } n\text{-bands} = M - 1 = nm - (n - 1)m' - 1 \quad (3.15)$$

which coincides with the maximum value of the Kac label r . For $\lambda > \pi/n$, there are no shaded n -bands. For $\lambda < \pi/n$, since $n' < n$ implies $\pi/n < \pi/n'$, it follows that for each $n' < n$ the number of shaded n' -bands is also given by $M(m, m', n') - 1 = n'm - (n' - 1)m' - 1$.

Following [6], we also use the sequences

$$h_a = \left\lfloor \frac{a(m' - m)}{m'} \right\rfloor = \left\lfloor \frac{a\lambda}{\pi} \right\rfloor = \# \text{ unshaded 1-bands below the height } a \quad (3.16)$$

The value of h_a remains unchanged within any shaded n -band. The value $h_a = 0, 1, 2, \dots$ thus labels, from the bottom, the contiguous shaded bands (independent of the width of the individual shaded bands) separated by unshaded 1-bands.

3.3.2 Fused RSOS ground state boundary conditions

The initial height a in the fused RSOS paths is to be identified with the Kac label s . We posit further that, in the sector (a, b, c) , (b, c) is a ground state boundary condition if the heights b and c lie within

the same shaded n -band $(\rho, \rho + n)$ (labelled by r), that is $b, c \in (\rho, \rho + n)$, and they are symmetrically placed about its center $\frac{1}{2}(b + c) = \rho + \frac{1}{2}n$. Defining

$$\ell = \frac{1}{2}[n + (-1)^{h_b}(b - c)] = 0, 1, 2, \dots, n, \quad \tilde{\ell} = \frac{1}{2}(n + b - c) = \begin{cases} \ell, & h_b \text{ even} \\ n - \ell, & h_b \text{ odd} \end{cases} \quad (3.17)$$

we see that $h_b = h_c$ and

$$s = a, \quad \rho = \frac{1}{2}(b + c - n), \quad b = \rho + \tilde{\ell}, \quad c = \rho + n - \tilde{\ell} \quad (3.18)$$

Given (m, m', n) , these relations allow to uniquely map back and forth between the boundary conditions (a, b, c) and the Kac label quantum numbers (r, s, ℓ) with $r = r^{m, m', n}(\rho)$. Boundary conditions (b, c) not satisfying these conditions are non-ground state boundary conditions.

3.4 Local energies and one-dimensional sums

In this section, we consider the local energy functions $H(d, a, b)$ and their associated one-dimensional sums. In particular, restricting to the interval $0 < \lambda < \pi/n$, we give exhaustive lists of the values of the local energies according to the shading of the internal bands for $n = 1, 2, 3$. As explained in Appendix B, not all patterns of shaded bands actually occur for $0 < \lambda < \pi/n$. Specifically, in this smaller interval considered in this paper, any n contiguous bands must have at most one unshaded 1-band. In the unitary cases ($m = m' - 1$), all of the 1-bands are shaded. Accordingly, in agreement with [21], we find that the local energy functions with all internal 1-bands shaded (that is 1-bands between $\text{Min}[d, a, b]$ and $\text{Max}[d, a, b]$) are given by

$$H(d, a, b) = \frac{1}{4}|b - d| \quad (3.19)$$

Moreover, the local energies possess reflection and height reversal symmetries

$$H(d, a, b) = H(b, a, d) = H(m' - d, m' - a, m' - b) \quad (3.20)$$

which are inherited from the face weights. Noting that the physical quantities of interest are unchanged if the local energy functions are shifted by an additive constant, we use this and the gauge freedom to ensure that

$$0 \leq H(d, a, b) \leq \frac{n}{2} \quad (3.21)$$

Lastly, we impose the ground state requirement

$$H(b, c, b) = H(c, b, c) = 0, \quad \text{whenever } (b, c) \text{ is a ground state boundary condition} \quad (3.22)$$

3.4.1 Local energy functions

Following Baxter, after fixing a suitable normalization and gauge g_a , the local energy functions $H(d, a, b)$ are given by the low-temperature limit

$$t = e^{-\varepsilon} \rightarrow 1, \quad u, \varepsilon \rightarrow 0, \quad u/\varepsilon \text{ fixed} \quad (3.23)$$

of the face weights (3.6)

$$W^{n, n} \left(\begin{matrix} d & c \\ a & b \end{matrix} \middle| u \right) \sim \frac{g_a g_c}{g_b g_d} w^{H(d, a, b)} \delta(a, c), \quad w = e^{-2\pi u/\varepsilon} \quad (3.24)$$

This limit is evaluated by performing a *conjugate modulus transformation* on the elliptic theta functions

$$\theta_1(u, t) = \left(\frac{\pi}{\varepsilon} \right)^{1/2} e^{-(u - \pi/2)^2/\varepsilon} E(w, p) \quad (3.25)$$

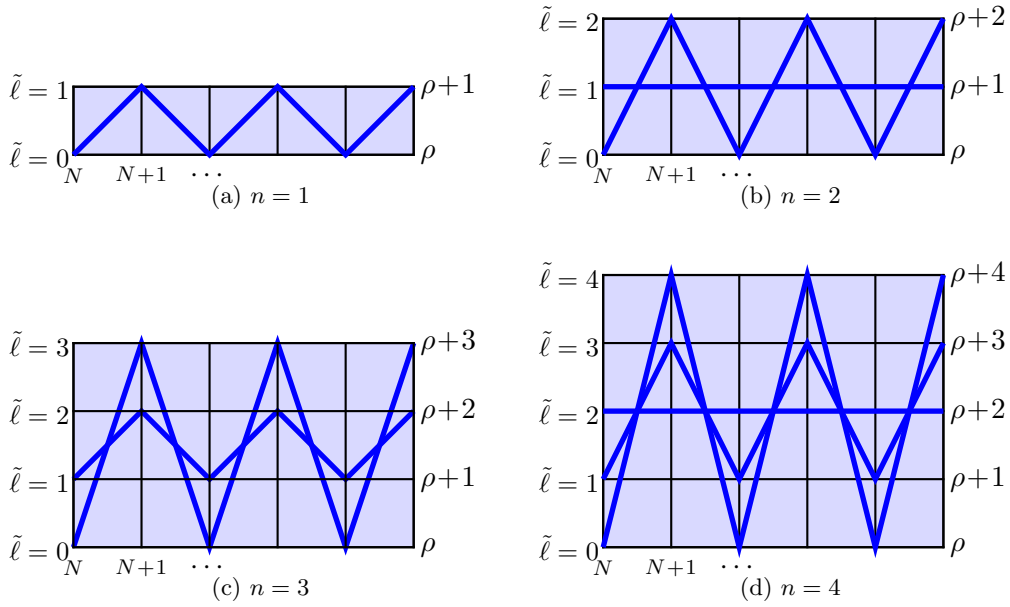


Figure 2: Extended ground state boundary conditions $(\sigma_N, \sigma_{N+1}) = (b, c) = (\rho + \tilde{\ell}, \rho + n - \tilde{\ell})$ for $\tilde{\ell} = 0, 1, \dots, \lfloor \frac{n}{2} \rfloor$ and $n = 1, 2, 3, 4$. The values of $\tilde{\ell}$ are shown on the left and the heights are shown on the right. The ground states for $\lfloor \frac{n}{2} \rfloor < \tilde{\ell} \leq n$ are obtained by applying the height reversal $\sigma_j \mapsto 2\rho + n - \sigma_j$ within the shaded n -band. In all cases, the local energies satisfy $H(b, c, b) = H(c, b, c) = 0$. Here $\tilde{\ell} = \ell$ or $n - \ell$ according to (3.17).

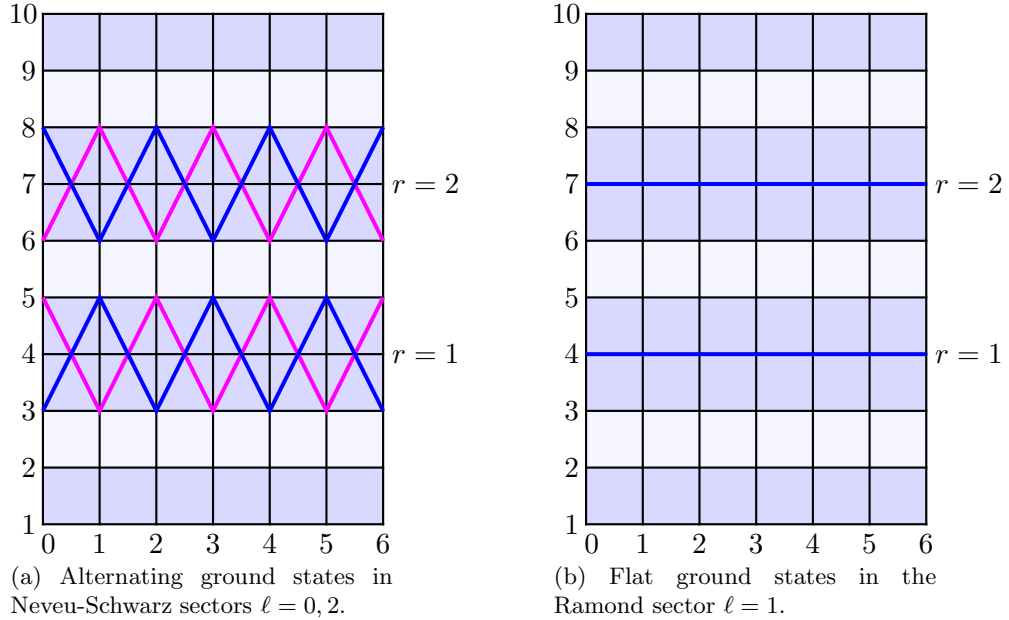


Figure 3: Extended ground state boundary conditions $(\sigma_N, \sigma_{N+1}) = (b, c) = (\rho + \tilde{\ell}, \rho + n - \tilde{\ell})$ for $\tilde{\ell} = 0, 1, \dots, n$ for the superconformal minimal model $\mathcal{M}(3, 11, 2)$ with $(m, m', n) = (7, 11, 2)$ and 2-bands at $\rho = 3, 6$ with $r = 1, 2$. Here $\tilde{\ell} = \ell$ or $n - \ell$ according to (3.17). The ground states are separated into Neveu-Schwarz ($\ell = 0, 2; r + s$ even) and Ramond ($\ell = 1; r + s$ odd) sectors.

where

$$E(w, p) = E(w) = \sum_{n=-\infty}^{\infty} (-1)^n p^{n(n-1)/2} w^n = \prod_{n=1}^{\infty} (1 - p^{n-1} w)(1 - p^n w^{-1})(1 - p^n) \quad (3.26)$$

with variables

$$w = e^{-2\pi u/\varepsilon}, \quad p = e^{-2\pi^2/\varepsilon}, \quad x = p^{\lambda/\pi} = e^{-2\pi\lambda/\varepsilon} \quad (3.27)$$

To evaluate the low-temperature limit $x \rightarrow 0$, or equivalently $p \rightarrow 0$, we use the following elementary properties of the E -functions

$$E(w, p) = E(p w^{-1}, p) = -w E(w^{-1}, p) \quad (3.28)$$

$$E(p^n w, p) = (-w)^{-n} p^{-n(n-1)/2} E(w, p) \quad (3.29)$$

$$\lim_{p \rightarrow 0} E(p^a w, p^b) = \begin{cases} 1, & 0 < a < b \\ 1 - w, & a = 0 \end{cases} \quad (3.30)$$

where n is an arbitrary integer. Using these properties, we deduce the further useful limit

$$\lim_{x \rightarrow 0} \frac{E(x^a w^{-1})}{E(x^a)} = w^{\lfloor a\lambda/\pi \rfloor} = w^{h_a} \quad (3.31)$$

3.4.2 Energy statistic and one-dimensional sums

The energy statistic and the associated one-dimensional sums were introduced by Baxter in the context of Corner Transfer Matrices (CTMs) [7, 31]. The energy statistic associated with a one-dimensional RSOS path $\sigma = \{\sigma_0, \sigma_1, \dots, \sigma_N, \sigma_{N+1}\}$ is

$$E(\sigma) = \sum_{j=1}^N j H(\sigma_{j-1}, \sigma_j, \sigma_{j+1}) \quad (3.32)$$

The associated one-dimensional sums are

$$X_{abc}^{(N)}(q) = \sum_{\sigma} q^{E(\sigma)} \quad (3.33)$$

where the sum is over all allowed RSOS paths satisfying the boundary conditions

$$(\sigma_0, \sigma_N, \sigma_{N+1}) = (a, b, c) \quad (3.34)$$

Due to the requirement (3.22), the ground state boundary condition (b, c) can be extended beyond $j = N + 1$ to infinity, without changing the energy statistic (3.32) associated to paths, simply by alternating σ_j between heights b and c for $j \geq N$. It is in this sense that the energy-weighted finite RSOS paths give a truncated set of conformal energies of the infinite system. Examples of extended ground states are shown in Figures 2 and 3.

The local energy function $H(\sigma_{j-1}, \sigma_j, \sigma_{j+1})$ is not unique. Its form is changed by incorporating the gauge factors $g_a = w^{\tilde{g}_a}$ in (3.24)

$$\begin{aligned} H'(\sigma_{j-1}, \sigma_j, \sigma_{j+1}) &= H(\sigma_{j-1}, \sigma_j, \sigma_{j+1}) + 2\tilde{g}_{\sigma_j} - \tilde{g}_{\sigma_{j-1}} - \tilde{g}_{\sigma_{j+1}} \\ &= H(\sigma_{j-1}, \sigma_j, \sigma_{j+1}) + (\tilde{g}_{\sigma_j} - \tilde{g}_{\sigma_{j-1}}) - (\tilde{g}_{\sigma_{j+1}} - \tilde{g}_{\sigma_j}) \end{aligned} \quad (3.35)$$

In a given sector with $(\sigma_0, \sigma_N, \sigma_{N+1}) = (a, b, c)$, it follows that

$$\begin{aligned} E'(\sigma) &= \sum_{j=1}^N j H'(\sigma_{j-1}, \sigma_j, \sigma_{j+1}) = E(\sigma) + \sum_{j=1}^N j (2\tilde{g}_{\sigma_j} - \tilde{g}_{\sigma_{j-1}} - \tilde{g}_{\sigma_{j+1}}) \\ &= E(\sigma) + [(N+1)\tilde{g}_b - N\tilde{g}_c - \tilde{g}_a] = E(\sigma) + N(\tilde{g}_b - \tilde{g}_c) + (\tilde{g}_b - \tilde{g}_a) \end{aligned} \quad (3.36)$$

independent of the path σ . Since this amounts to a shift in the ground state energy by a constant amount, the two energy statistics are equivalent.

Summing over allowed neighbours of b , the one-dimensional sums satisfy the linear recursion relations

$$X_{abc}^{(N)}(q) = \sum_{d \sim b} q^{NH(d,b,c)} X_{adb}^{(N-1)}(q) \quad (3.37)$$

subject to the initial and boundary conditions

$$X_{abc}^{(0)}(q) = \delta(a, b), \quad X_{a0c}^{(N)}(q) = X_{a\{m'\}c}^{(N)}(q) = 0 \quad (3.38)$$

where b and c are neighbours. This data uniquely determines $X_{abc}^{(N)}(q)$. Our conjecture is that the one-dimensional sums coincide with finitized branching functions up to the leading powers of q

$$X_{abc}^{(N)}(q) \cong b_{r,s,\ell}^{M,M',n;(N)}(q), \quad \lim_{N \rightarrow \infty} X_{abc}^{(N)}(q) \cong b_{r,s,\ell}^{M,M',n}(q) \quad (3.39)$$

Duality (3.8) is implemented on finite one-dimensional sums by $q \leftrightarrow q^{-1}$ or $H(a, b, c) \leftrightarrow -H(a, b, c)$ and interchanges the intervals $\lambda \in (0, \pi/2)$ and $\lambda \in (\pi/2, \pi)$.

3.4.3 $n = 1$ local energies

Working in the gauge $g_a = 1$ for $n = 1$, the local energy function obtained by Forrester-Baxter [6] is

$$H^{\text{FB}}(a, a \mp 1, a) = \pm h_a \quad (3.40a)$$

$$H^{\text{FB}}(a \pm 1, a, a \mp 1) = \frac{1}{2} \quad (3.40b)$$

where h_a is given by (3.16).

Starting with $H^{\text{FB}}(a, b, c)$, we apply a specific additive gauge transformation given by

$$G_a - G_b = \frac{1}{4}(a - b)(h_a + h_b), \quad b = a \pm 1; \quad G_a = \frac{1}{4} \sum_{c=1}^a (h_c + h_{c-1}) + G_0 \quad (3.41)$$

where we choose $G_0 = 0$ and solve by iterating with $b = a - 1$. This gives the equivalent gauged local energy function

$$H(a+1, a, a+1) = \frac{1}{2}(h_{a+1} - h_a) \quad (3.42a)$$

$$H(a-1, a, a-1) = \frac{1}{2}(h_a - h_{a-1}) \quad (3.42b)$$

$$H(a \pm 1, a, a \mp 1) = \frac{1}{2} - \frac{1}{4}(h_{a+1} - h_{a-1}) \quad (3.42c)$$

where

$$h_{a+1} - h_a = \begin{cases} 0, & a \text{ labels a ground state: } (a, a+1) \text{ is a shaded band} \\ 1, & a \text{ is not a ground state: } (a, a+1) \text{ is not a shaded band} \end{cases} \quad (3.43)$$

It follows that $H(a, b, c)$ is nonnegative with values shown in Figure 4. This particular choice of gauge respects the duality

$$m \mapsto m' - m, \quad \text{shaded bands} \leftrightarrow \text{unshaded bands}, \quad H^{m,m'}(a, b, c) \mapsto \frac{1}{2} - H^{m'-m,m'}(a, b, c) \quad (3.44)$$

Anticipating the cases $n = 2, 3$, we further note that

$$h_{a+n} - h_a = \sum_{k=0}^{n-1} (h_{a+k+1} - h_{a+k}) = \begin{cases} 0, & (a, a+n) \text{ is a shaded } n\text{-band} \\ 1, & (a, a+n) \text{ is not a shaded } n\text{-band} \end{cases} \quad (3.45)$$

since, from Appendix B, any n -band contains at most one unshaded 1-band.

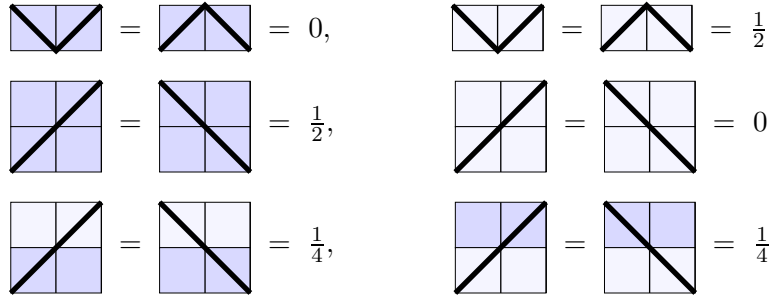


Figure 4: The gauged local energies of the $n = 1$ RSOS models in the interval $0 < \lambda < \pi$. These local energies satisfy duality $H^{m,m'}(a,b,c) = \frac{1}{2} - H^{m'-m,m'}(a,b,c)$ under interchange of shaded and unshaded bands. In this gauge, the local energies take the values $0, \frac{1}{4}, \frac{1}{2}$.

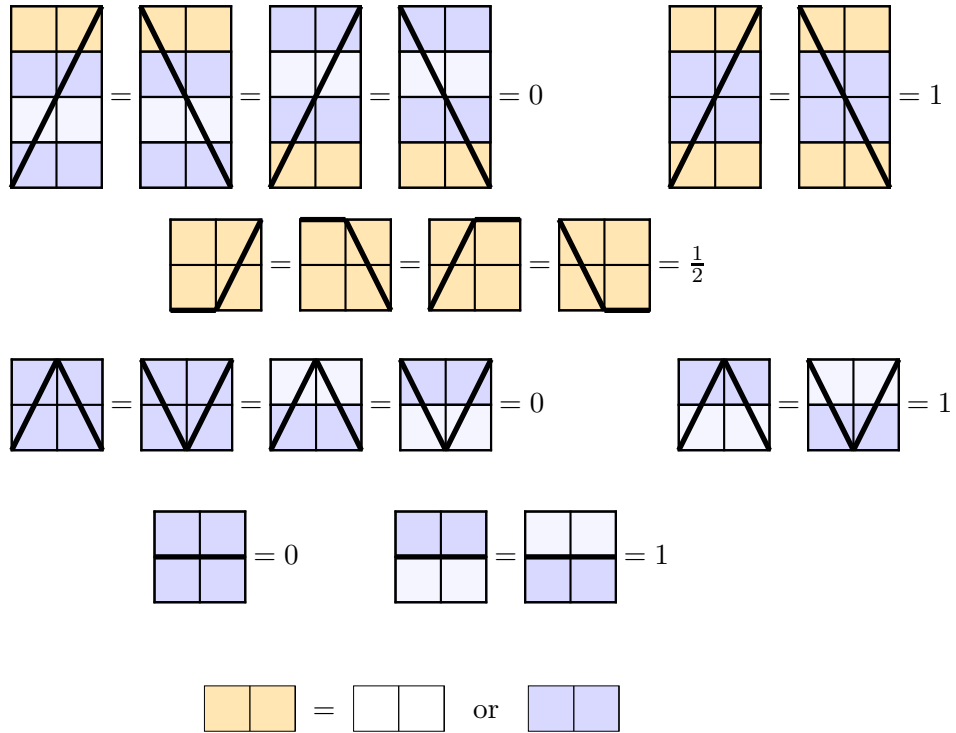


Figure 5: The gauged local energies of the $n = 2$ RSOS models in the interval $0 < \lambda < \pi/2$. The light orange bands indicate that the result holds whether the band is shaded or unshaded. As shown in Appendix B, contiguous unshaded bands do not occur in the interval $0 < \lambda < \pi/2$. In this gauge, the local energies take the values $0, \frac{1}{2}, 1$.

3.4.4 $n = 2$ local energies

For $n = 2$, the low temperature limit is similarly obtained by taking $x \rightarrow 0$. After a renormalization by $\exp(2u(\lambda - u)/\varepsilon)$ and a conjugate modulus transformation, the diagonal $n = 2$ face weights can be rewritten as in (D.1) with the multiplicative gauge

$$g_a = w^{a(a\lambda - \pi)/4\pi} \quad (3.46)$$

The local energies are found to be

$$H(a \pm 2, a, a \mp 2) = 1 \quad (3.47a)$$

$$H(a \pm 2, a, a) = H(a, a, a \pm 2) = \frac{1}{2} \pm h_{a\pm 1} \quad (3.47b)$$

$$H(a, a \pm 2, a) = \mp(h_a + h_{a\pm 1}) \quad (3.47c)$$

$$H(a, a, a) = \begin{cases} 0, & h_{a-1} = h_a = h_{a+1} \\ 1, & \text{otherwise} \end{cases} \quad (3.47d)$$

We apply a further additive gauge transformation G_a that satisfies

$$G_a = \begin{cases} h_1 + h_3 + \dots h_{a-1}, & a \text{ even} \\ h_2 + h_4 + \dots h_{a-1}, & a \text{ odd} \end{cases} \quad G_{a+1} - G_{a-1} = h_a \quad (3.48)$$

This transformation is implemented more neatly by defining $G(a, b) = G_b - G_a$ so that

$$H'(a, b, c) = H(a, b, c) + G(a, b) - G(b, c) \geq 0, \quad G(a, b) = \frac{1}{2}(b - a)h_{\frac{a+b}{2}} \quad (3.49)$$

Rewriting the local energies using this new gauge, and omitting the prime, gives the local energies

$$H(a \pm 2, a, a \mp 2) = h_{a-1} - h_{a+1} + 1 \quad (3.50a)$$

$$H(a \pm 2, a, a) = H(a, a, a \pm 2) = \frac{1}{2} \quad (3.50b)$$

$$H(a, a \pm 2, a) = \pm(h_{a\pm 1} - h_a) \quad (3.50c)$$

$$H(a, a, a) = \begin{cases} 0, & h_{a-1} = h_a = h_{a+1} \\ 1, & \text{otherwise} \end{cases} \quad (3.50d)$$

These local energies take the values 0, 1/2 or 1 as shown in Figure 5.

3.4.5 $n = 3$ local energies

For $n = 3$, we follow the same procedure as in the $n = 2$ case with the same multiplicative gauge $g_a = w^{a(a\lambda - \pi)/4\pi}$. We perform a conjugate modulus transformation on the weights and further normalize by $\exp(3u(\lambda - u)/\varepsilon)$ to obtain the conjugate modulus face weights as written in (D.2).

Taking the low-temperature limit $x \rightarrow 0$ gives the local energy functions

$$H(a \pm 3, a, a \pm 3) = \pm(h_{a\pm 1} + h_{a\pm 2} + h_{a\pm 3}) \quad (3.51a)$$

$$H(a \pm 3, a, a \pm 1) = H(a \pm 1, a, a \pm 3) = \frac{1}{2} \pm (h_{a\pm 1} + h_{a\pm 2}) \quad (3.51b)$$

$$H(a \pm 3, a, a \mp 1) = H(a \mp 1, a, a \pm 3) = 1 \pm h_{a\pm 1} \quad (3.51c)$$

$$H(a \pm 3, a, a \mp 3) = \frac{3}{2} \quad (3.51d)$$

$$H(a \pm 1, a, a \pm 1) = \begin{cases} 1 \pm h_{a\pm 1}, & h_{a+2} = h_{a+1} = h_{a-1} + 1 = h_{a-2} + 1 \\ \pm h_{a\pm 2}, & \text{otherwise} \end{cases} \quad (3.51e)$$

$$H(a \pm 1, a, a \mp 1) = \frac{1}{2} + h_{a+1} - h_{a-1} \quad (3.51f)$$

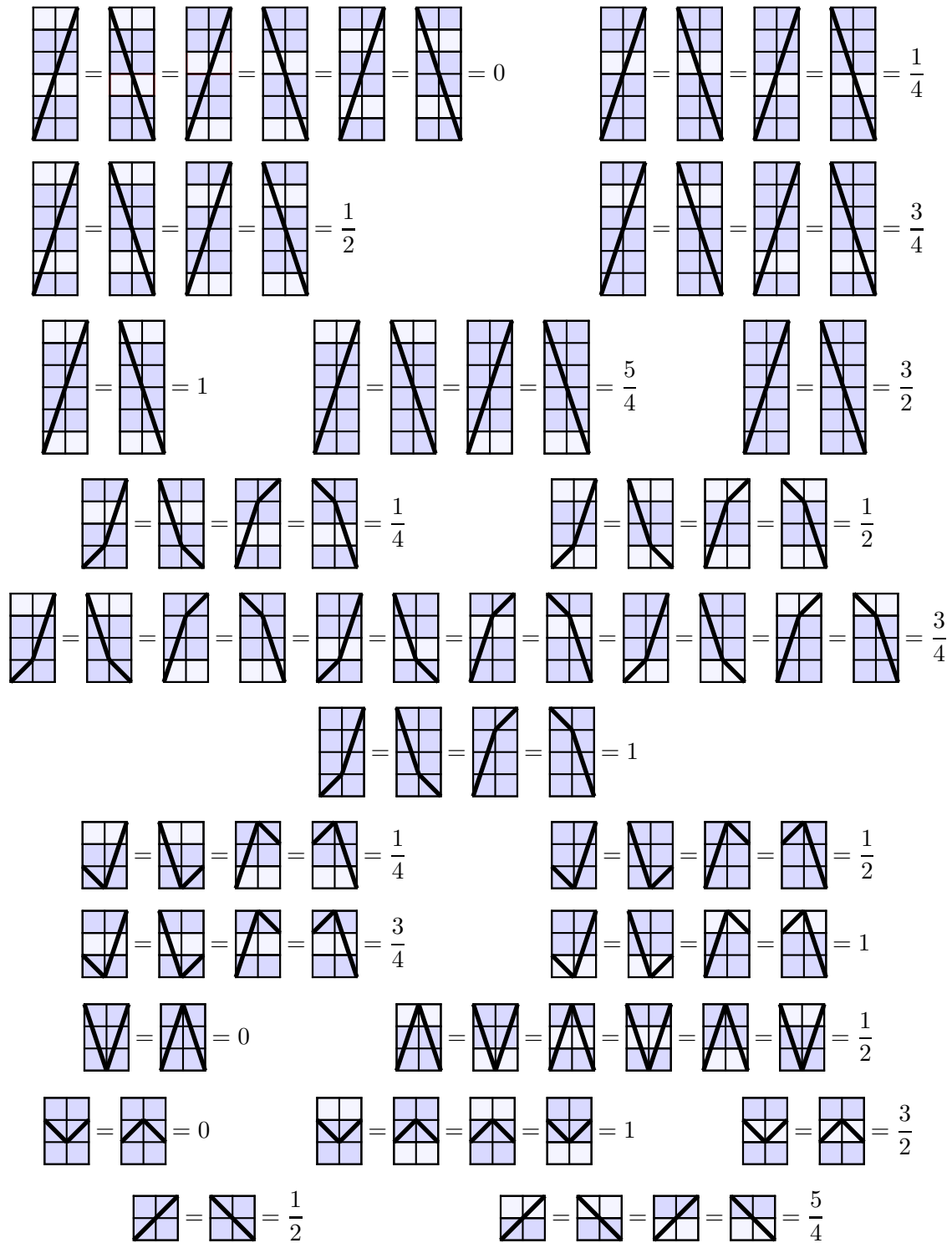


Figure 6: The gauged local energies of the $n=3$ RSOS models in the interval $0 < \lambda < \pi/3$. In this gauge, the local energies take the values $0, \frac{1}{4}, \frac{1}{2}, \frac{3}{4}, 1, \frac{5}{4}, \frac{3}{2}$.

We impose an additive gauge G_a which assures the local energy functions are non-negative

$$H'(a, b, c) = H(a, b, c) + 2G_b - G_a - G_c \geq 0 \quad (3.52)$$

One such gauge is

$$G_a = \frac{1}{4} \sum_{k=1}^{a-1} (h_{k+1} + h_k), \quad G_{a+1} - G_a = \frac{1}{4} (h_{a+1} + h_a) \quad (3.53)$$

resulting in the local energies

$$H(a \pm 3, a, a \pm 3) = \pm \frac{1}{2} (h_{a \pm 3} - h_a) \quad (3.54a)$$

$$H(a \pm 3, a, a \pm 1) = H(a \pm 1, a, a \pm 3) = \frac{1}{2} \pm \frac{1}{4} (-2h_a + h_{a \pm 1} + 2h_{a \pm 2} - h_{a \pm 3}) \quad (3.54b)$$

$$H(a \pm 3, a, a \mp 1) = H(a \mp 1, a, a \pm 3) = 1 \pm \frac{1}{4} (h_{a \mp 1} + 2h_{a \pm 1} - 2h_{a \pm 2} - h_{a \pm 3}) \quad (3.54c)$$

$$H(a \pm 3, a, a \mp 3) = \frac{3}{2} + \frac{1}{4} (h_{a-3} + 2h_{a-2} + 2h_{a-1} - 2h_{a+1} - 2h_{a+2} - h_{a+3}) \quad (3.54d)$$

$$H(a \pm 1, a, a \pm 1) = \begin{cases} \pm (h_{a \pm 2} - h_{a \pm 1}), & h_{a+1} = h_a = h_{a-1} \\ \pm \frac{1}{2} (h_{a \pm 1} - h_a) + 1, & h_{a+1} = h_{a-1} + 1 \end{cases} \quad (3.54e)$$

$$H(a \pm 1, a, a \mp 1) = \frac{1}{2} + \frac{3}{4} (h_{a+1} - h_{a-1}) \quad (3.54f)$$

Evaluating these local energy functions on all possible two step paths and band shadings gives the local energies shown in Figure 6.

4 Conjectured Finitized Bosonic Branching Functions

4.1 Finitized bosonic branching functions

In this section we present conjectured finitized bosonic branching functions for the nonunitary minimal cosets $\mathcal{M}(M, M', n)$, generalizing the unitary case considered by Schilling [30]. For simplicity, we assume throughout that the system size N is even so that $b - a$ is even. The finitized bosonic branching functions are written in terms of q -multinomials [30, 35]. We use the notation $T_\ell^{(n)}(N, \mu)$ as in (2.12) of Schilling [30]

$$T_\ell^{(n)}(N, \mu) = \sum'_{\tilde{v} \in \mathbb{Z}_{\geq 0}^{n+1}} q^{v C^{-1} v - e_\ell C^{-1} v} (q)_N \prod_{i=0}^n \frac{1}{(q)_{v_i}} \quad (4.1)$$

where $\tilde{v} = (v_0, v_1, \dots, v_n)$, $v = (v_1, v_2, \dots, v_{n-1})$ are integer vectors and the primed sum indicates a sum over all $v_i \in \mathbb{Z}_{\geq 0}$, $i = 0, 1, 2, \dots, n$ subject to the constraints

$$v_0 = \frac{N}{2} - \frac{\mu}{n} - e_1 C^{-1} v, \quad v_n = \frac{N}{2} + \frac{\mu}{n} - e_{n-1} C^{-1} v, \quad \mu = -\frac{nN}{2}, -\frac{nN}{2} + 1, \dots, \frac{nN}{2} \quad (4.2)$$

The matrix C^{-1} in the quadratic form is the inverse of the Cartan matrix C with entries $C_{a,b} = 2 - \delta(a, b+1) - \delta(a, b-1)$ and the vectors $\{e_j\}_{j=1}^{n-1}$ are $(n-1)$ -dimensional standard basis vectors

$$C_{i,j}^{-1} = \begin{cases} (n-i)j/n, & j \leq i \\ (n-j)i/n, & j > i \end{cases} \quad (e_i)_j = \begin{cases} \delta(i, j), & i = 1, 2, \dots, n-1 \\ 0, & \text{otherwise} \end{cases} \quad (4.3)$$

Alternatively, the q -multinomials can be defined recursively

$$T_\ell^{(n)}(N, \mu) = \sum_{k=0}^{\ell-1} q^{(\ell-k)(\frac{N}{2} + \frac{\mu}{n})} T_{n-k}^{(n)}(N-1, \frac{n}{2} + \mu - k) + \sum_{k=\ell}^n q^{(k-\ell)(\frac{N}{2} - \frac{\mu}{n})} T_{n-k}^{(n)}(N-1, \frac{n}{2} + \mu - k) \quad (4.4)$$

subject to

$$T_\ell^{(n)}(0, \mu) = \delta(\mu, 0) \quad (4.5)$$

Explicitly, generalizing Schilling [30], our conjectured finitized bosonic branching functions are

$$b_{r,s,\ell}^{M,M',n;(N)}(q) \cong \sum_{j=-\infty}^{\infty} \left\{ q^{\frac{j}{n}(jMM'+M'r-Ms)} T_{(n+b-c)/2}^{(n)}(N, \frac{1}{2}(b-a) + jM') \right. \\ \left. - q^{\frac{1}{n}(jM+r)(jM'+s)} T_{(n+b-c)/2}^{(n)}(N, \frac{1}{2}(b+a) + jM') \right\} \quad (4.6)$$

where the symbol \cong indicates that the identification holds up to leading powers of q . In this formula

$$M = nm - (n-1)m', \quad M' = m', \quad \ell = \frac{1}{2}[n + (-1)^{h_b}(b-c)] \quad (4.7)$$

Observe that $\gcd(\frac{M'-M}{n}, M') = \gcd(m'-m, m') = 1$ whenever $\gcd(m, m') = 1$. In the unitary case, all the bands are shaded with $m = m' - 1$, $\lambda = \frac{\pi}{n}$, $M = m' - n$, $h_a \equiv 0$ so this formula reduces to the formula in Schilling [30]. If h_b is odd, we interchange b and c . After this interchange, if it is required, the quantum numbers and boundary conditions are related by

$$s = a, \quad \rho = \frac{1}{2}(b+c-n), \quad \ell = \frac{1}{2}(n+b-c) = b - \rho \quad (4.8)$$

with r uniquely determined by $r = r(\rho) = r^{m,m',n}(\rho)$. For many minimal models $\mathcal{M}(M, M', n)$ and exhaustive boundary conditions, we have checked symbolically in Mathematica that the conjecture correctly reproduces the one-dimensional sums, up to the leading powers of q , for $n = 1, 2, 3$ out to system size $N = 14$. In every case, as guaranteed by the one-dimensional sums, the resulting q -polynomials have nonnegative coefficients.

Finitizations similar to (4.6), but involving q -supernomials and multiple finitization parameters $\mathbf{L} = (L_1, L_2, \dots, L_n)$, have been proposed by Schilling and Warnaar [58]. Setting $L_i = N\delta(i, n)$ for $i = 1, 2, \dots, n$ and $\ell = 0$, the q -supernomials reduce to the q -multinomials $T_0^{(n)}(N, \mu)$. Relaxing the Takahashi length restrictions on a, b in these cases, it follows that the finitizations of [58] coincide with (4.6). In these and other cases, these authors have identified the associated fermionic forms and proven bosonic equals fermionic type identities. However, a simple relationship between the q -supernomial and q -multinomial finitizations in the sectors with $\ell \neq 0, n$ is not known.

Setting $q = 1$ in (4.6) gives the correct counting of states. To take the limit $N \rightarrow \infty$ to obtain the full branching functions, we use (2.16) of Schilling [30]

$$T_\ell^{(n)}(\mu) = \lim_{N \rightarrow \infty, N \text{ even}} T_\ell^{(n)}(N, \mu) = \frac{1}{(q)_\infty} \sum_{v \in \mathbb{Z}_{\geq 0}^{n-1}, \frac{\mu}{n} + e_1 C^{-1} v \in \mathbb{Z}} q^{vC^{-1}v - e_\ell C^{-1}v} \prod_{i=1}^{n-1} \frac{1}{(q)_{v_i}} \quad (4.9)$$

which only depends on $\mu \bmod n$ with $T_\ell^{(n)}(\mu) = T_\ell^{(n)}(\ell - \mu)$. We therefore find

$$b_{r,s,\ell}^{M,M',n}(q) \cong \sum_{\substack{0 \leq m \leq n/2 \\ m = \ell/2 \bmod 1}} T_\ell^{(n)}(m + \frac{1}{2}\ell) \\ \times \left[\sum_{\substack{j \in \mathbb{Z} \\ m_{r-s}(j) = \pm m \bmod n}} q^{\frac{j}{n}(jMM'+M'r-Ms)} - \sum_{\substack{j \in \mathbb{Z} \\ m_{r+s}(j) = \pm m \bmod n}} q^{\frac{1}{n}(jM+r)(jM'+s)} \right] \quad (4.10)$$

where

$$m_a(j) := a/2 + jM' \quad (4.11)$$

and we use (4.8) and

$$\frac{1}{2}(b \mp a) + jM' = \frac{1}{2}(\rho \mp s) + jM' + \frac{1}{2}\ell = m + \frac{1}{2}\ell \bmod n, \quad \rho = r \bmod n \quad (4.12)$$

We prove the result $\rho = r \bmod n$ in Appendix B. Note that with N even, from (4.10) to (4.12), $r - s + \ell$ must be even. Also, using (4.8), $b - a = \rho - s + \ell$ is also even. Note also that, if n is odd, then b and c have opposite parities and it is only possible to get from a to one of b or c in an even number of steps N . So b is uniquely determined by the condition $b - a = 0 \bmod 2$ and it is the b in (4.8). If n is even, it is possible to get to either b or c in N steps. In this case, interchanging b and c is equivalent to $\ell \leftrightarrow n - \ell$.

Lastly, to obtain the branching functions in the form (2.15), we use (3.30) of Schilling [30] which asserts that $T_\ell^{(n)}(m + \frac{1}{2}\ell) \cong c_{2m}^\ell(q)$. Explicitly, up to leading powers of q , $T_\ell^{(n)}(m + \frac{1}{2}\ell)$ is the \mathbb{Z}_n parafermionic string function

$$c_{2m}^\ell(q) = q^{\frac{\hat{c}}{24} - \frac{1}{4n} + \frac{n}{4MM'} + \frac{\ell+1}{2n} - \frac{(\ell+1)^2}{2n(n+2)} - \frac{1}{8}} T_\ell^{(n)}(m + \frac{1}{2}\ell), \quad \ell = 0, 1, \dots, n \quad (4.13)$$

with

$$\hat{c} = 1 - \frac{6n}{MM'} + \frac{2(n-1)}{n+2} \quad (4.14)$$

Note that, in this formula, m can take half-integer values and $2m$ is the parafermionic index.

4.2 Logarithmic limit and finitized Kac characters

Following [51] and [49], the Kac characters of the logarithmic minimal models $\mathcal{LM}(p, p')$ [48] and their $n \times n$ fusion hierarchies [50] are given by taking the *logarithmic limit*. Symbolically

$$\lim_{m, m' \rightarrow \infty, \frac{m'}{m} \rightarrow \frac{p'}{p} +} \mathcal{M}(M, M', n) = \mathcal{LM}(P, P', n), \quad 1 \leq p < p', \quad p, p' \text{ coprime} \quad (4.15)$$

where

$$(M, M') = (nm - (n-1)m', m'), \quad (P, P') = (np - (n-1)p', p') \quad (4.16)$$

The (one-sided) limit is taken through coprime pairs (m, m') with $\frac{m'}{m} > \frac{p'}{p}$. The one-sided limit is needed to ensure the sequences of minimal model ground states converge to the correct logarithmic minimal model ground states. Formally, the logarithmic limit is taken in the continuum scaling limit after the thermodynamic limit. The equality indicates the identification of the spectra of the chiral CFTs. In principle, the Jordan cells appearing in the reducible yet indecomposable representations of the logarithmic minimal models should emerge in this limit but there are subtleties [51].

Since finitized characters give the spectrum generating functions for finite truncated sets of conformal energies, the logarithmic limit can be applied directly to finitized characters. Assuming $0 < |q| < 1$ and taking the logarithmic limit of the finitized branching functions (4.6), we find that up to leading powers of q , the finitized Kac characters are

$$\chi_{r,s,\ell}^{P,P',n;(N)}(q) \cong T_{(n+b-c)/2}^{(n)}(N, \frac{1}{2}(b-a)) - q^{\frac{1}{n}rs} T_{(n+b-c)/2}^{(n)}(N, \frac{1}{2}(b+a)) \quad (4.17)$$

where the quantum numbers are related to the boundary conditions by (3.17) and (3.18) with $h_a = \lfloor \frac{a(p'-p)}{p'} \rfloor$. Taking the thermodynamic limit gives

$$\chi_{r,s,\ell}^{P,P',n}(q) = \lim_{N \rightarrow \infty, N \text{ even}} \chi_{r,s,\ell}^{n;(N)}(q) \cong T_{(n+b-c)/2}^{(n)}(\frac{1}{2}(b-a)) - q^{\frac{1}{n}rs} T_{(n+b-c)/2}^{(n)}(\frac{1}{2}(b+a)) \quad (4.18)$$

or equivalently

$$\chi_{r,s,\ell}^{P,P',n}(q) \cong c_{r-s}^\ell - q^{\frac{1}{n}rs} c_{r+s}^\ell, \quad r, s \in \mathbb{N}, \quad \ell = 0, 1, \dots, n \quad (4.19)$$

Since the string functions vanish for $r + s + \ell$ odd, we must have $r + s = \ell \bmod 2$. The dependence on P, P' only enters through the leading powers of q as specified in [49]. For the logarithmic superconformal minimal models with $n = 2$ and $r = 1$, the finitized Kac characters agree with those of [50]. In this case, the counting of states given by trinomials reduces to generalized Motzkin and Riordan numbers in accord with the counting of the fused Temperley-Lieb link states.

5 Conclusion

In this paper we conjecture the identification (1.1), in the continuum scaling limit, of the $n \times n$ fused RSOS(m, m') lattice models with the higher-level minimal model cosets $\mathcal{M}(M, M', n)$ at fractional level $k = nM/(M' - M) - 2$ with $(M, M') = (nm - (n-1)m', m')$. This implies that the central charges of the $n \times n$ fused RSOS(m, m') models are

$$\mathcal{M}(M, M', n) : \quad c = c^{m, m', n} = \frac{3n}{n+2} \left[1 - \frac{2(n+2)(m' - m)^2}{m'(mn - m'(n-1))} \right] \quad (5.1)$$

The conjecture agrees with known results in the unitary cases ($m = m' - 1$). It is also supported in nonunitary cases ($2 \leq m \leq m' - 2$) by our explicit calculation of Baxter's one-dimensional sums for $n = 1, 2, 3$. Specifically, up to leading powers of q , we find that the one-dimensional sums give finitized branching functions. Indeed in many cases, using Mathematica out to system size $N = 14$, the resulting q -series are confirmed to converge towards the full branching functions.

Separately, generalizing the work of Schilling [30], the bosonic forms of the finitized branching functions (4.6) are conjectured for all nonunitary cases with $n \geq 1$. These finitized bosonic forms give the correct counting of states and reproduce the full branching functions in the thermodynamic limit $N \rightarrow \infty$. The explicit form of these finitized bosonic branching functions allows us to take the logarithmic limit. In this way, conjectured bosonic forms of the finitized Kac characters (4.17) are obtained for the higher-level fused logarithmic minimal models $\mathcal{LM}(P, P', n)$ thus extending the recent conjectures [50] restricted to the $n = 2$ logarithmic superconformal minimal models $\mathcal{LM}(P, P', 2)$.

All of the cosets (5.1) are realized with $\frac{n-1}{n} m' < m < m'$ corresponding to the interval $0 < \lambda < \pi/n$. Outside of this interval, there are no shaded n -bands to support the level- n ground states. It would therefore be of interest to extend the considerations of this paper to the full interval $0 < \lambda < \pi$. The level of rigour could also be improved by calculating, in the low-temperature limit, the local energies $H(a, b, c)$ valid for all n in a common gauge. It should then be possible to extend the proof of Schilling [30] to rigorously establish the equality of the one-dimensional sums with the finitized bosonic branching functions. We hope to return to these issues in a later paper.

Acknowledgments

This paper is dedicated to Rodney Baxter on the occasion of his 75th birthday. Elena Tartaglia is supported by an Australian Postgraduate Award. We thank Ole Warnaar for helpful comments and encouragement.

A Elliptic Functions

We summarize the definitions and properties of the elliptic functions used throughout this paper. The standard elliptic theta function $\vartheta_1(u, t)$ [56] is

$$\vartheta_1(u, t) = 2t^{1/4} \sin u \prod_{n=1}^{\infty} (1 - 2t^{2n} \cos 2u + t^{4n})(1 - t^{2n}) \quad (A.1)$$

Its conjugate modulus transformation is

$$\vartheta_1(u, e^{-\varepsilon}) = \sqrt{\frac{\pi}{\varepsilon}} e^{-(u-\pi/2)^2/\varepsilon} E(e^{-2\pi u/\varepsilon}, e^{-2\pi^2/\varepsilon}) \quad (A.2)$$

where

$$E(w, p) = \sum_{k=-\infty}^{\infty} (-1)^k p^{k(k-1)/2} w^k = \prod_{n=1}^{\infty} (1 - p^{n-1}w)(1 - p^n w^{-1})(1 - p^n) \quad (A.3)$$

The elliptic $\vartheta_1(u) = \vartheta_1(u, t)$ function satisfies the fundamental identity

$$\begin{aligned} \vartheta_1(u+x)\vartheta_1(u-x)\vartheta_1(v+y)\vartheta_1(v-y) - \vartheta_1(u+y)\vartheta_1(u-y)\vartheta_1(v+x)\vartheta_1(v-x) \\ = \vartheta_1(x-y)\vartheta_1(x+y)\vartheta_1(u+v)\vartheta_1(u-v) \end{aligned} \quad (\text{A.4})$$

B Counting of Contiguous Shaded Bands

B.1 Counting of shaded n -bands

Fix m and m' with $2 \leq m < m'$, $\gcd(m, m') = 1$ and consider a walk on the $A_{m'-1}$ Dynkin diagram. The bands $(a, a+1)$ at heights $a = \lfloor \frac{rm'}{m} \rfloor$ are shaded while the other bands are unshaded. An n -band consists of n contiguous bands, where each band is shaded or unshaded. If all the bands in an n -band are shaded, we call it a *shaded n -band*. If all the bands in an n -band are unshaded, we call it an *unshaded n -band*. Otherwise, we call it a *mixed n -band*.

Let us assume that $\lambda = (m' - m)\pi/m' < \pi/n$, that is,

$$nm - (n-1)m' > 0 \quad (\text{B.1})$$

and define

$$s_n := \# \text{ shaded } n\text{-bands} \quad (\text{B.2})$$

$$t_n := \# \text{ } n\text{-bands with exactly one unshaded 1-band} \quad (\text{B.3})$$

In this section, we prove that the number s_n of shaded n -bands is

$$s_n = M - 1 = nm - (n-1)m' - 1 \quad (\text{B.4})$$

More specifically, we show that

$$\# \text{ 1-bands} = m' - 2 = s_n + t_n + n - 1 \quad (\text{B.5a})$$

$$t_n = n \times \# \text{ unshaded 1-bands} = n(m' - m - 1) \quad (\text{B.5b})$$

Solving gives the required result (B.4).

We will need the elementary properties of floor functions

$$\lfloor n+x \rfloor = n + \lfloor x \rfloor, \quad \lfloor -x \rfloor = -\lceil x \rceil = -1 - \lfloor x \rfloor, \quad n \in \mathbb{Z}, x, y \in \mathbb{R} \quad (\text{B.6})$$

Using these, we obtain the two implications

$$\lfloor x \rfloor - \lfloor y \rfloor = n \Rightarrow n-1 < x-y < n+1, \quad \lfloor x \rfloor - \lfloor y \rfloor \leq n \Rightarrow x-y < n+1 \quad (\text{B.7})$$

To see the first result, let $x = \lfloor x \rfloor + r_x$, $y = \lfloor y \rfloor + r_y$ where $0 \leq r_x, r_y < 1$. Since $\lfloor x \rfloor - \lfloor y \rfloor = n$, we find

$$x-y = n + r_x - r_y, \quad -1 < r_x - r_y < 1 \quad (\text{B.8})$$

which gives the required bounds on $x-y$. The second result follows easily from the first. If $\lfloor x \rfloor - \lfloor y \rfloor = n$, then this follows from the first result. If not, then there must exist an integer $k \leq n-1$ such that $\lfloor x \rfloor - \lfloor y \rfloor = k$. We can then apply the first result to obtain $x-y < k+1 \leq n$.

Next we use these properties of floor functions to prove two preliminary results. The first preliminary result is that there are only two possible types of n -bands: shaded n -bands and n -bands with exactly one unshaded 1-band. Setting

$$h_{a+1} - h_a = \begin{cases} 0, & (a, a+1) \text{ shaded} \\ 1, & (a, a+1) \text{ unshaded} \end{cases} \quad h_a = \left\lfloor \frac{a(m'-m)}{m'} \right\rfloor \quad (\text{B.9})$$

this is equivalent to showing that for all n -bands $(a, a + n)$

$$0 \leq h_{a+n} - h_a = 0, 1 \quad (\text{B.10})$$

Assuming the converse, that is $h_{a+n} - h_a \geq 2$ for some n -band starting at height a , we use properties (B.6) to show

$$\begin{aligned} 2 \leq h_{a+n} - h_a &= \left\lfloor (a+n) \frac{(m'-m)}{m'} \right\rfloor - \left\lfloor a \frac{(m'-m)}{m'} \right\rfloor = a+n-1 - \left\lfloor (a+n) \frac{m}{m'} \right\rfloor - a+1 + \left\lfloor a \frac{m}{m'} \right\rfloor \\ &= n - \left\lfloor (a+n) \frac{m}{m'} \right\rfloor + \left\lfloor a \frac{m}{m'} \right\rfloor \end{aligned} \quad (\text{B.11})$$

Rearranging and applying the second property of (B.7) gives

$$\left\lfloor (a+n) \frac{m}{m'} \right\rfloor - \left\lfloor a \frac{m}{m'} \right\rfloor \leq n-2 \Rightarrow (a+n) \frac{m}{m'} - a \frac{m}{m'} < n-1 \Rightarrow nm - (n-1)m' < 0 \quad (\text{B.12})$$

which directly contradicts assumption (B.1).

The second preliminary result needed is that, for $n \geq 2$, there are always $n-1$ shaded 1-bands at the top and bottom of the $A_{m'-1}$ diagram. To show that there are always $n-1$ shaded 1-bands at the bottom, we use (B.6) and consider

$$0 \leq h_n - h_1 = h_n = \left\lfloor n \frac{(m'-m)}{m'} \right\rfloor = n-1 - \left\lfloor \frac{nm}{m'} \right\rfloor \quad (\text{B.13})$$

But now, from (B.1)

$$\frac{nm}{m'} > n-1 \Rightarrow \left\lfloor \frac{nm}{m'} \right\rfloor \geq n-1 \Rightarrow h_n - h_1 \leq 0 \quad (\text{B.14})$$

We conclude that $h_n - h_1 = 0$. A similar calculation shows that $h_{m'-1} = h_{m'-n}$ and proves that there are always $n-1$ shaded 1-bands at the top of the diagram.

Finally, we derive (B.5). We show that (B.5b) is true in two steps. Firstly,

$$t_n := \# n\text{-bands with exactly one unshaded 1-band} = n \times \# \text{ unshaded 1-bands} \quad (\text{B.15})$$

since, by scanning up the $A_{m'-1}$ diagram from bottom to top and looking at each consecutive n -band, each time there is an unshaded 1-band, it gets counted exactly n times. This is because there is only at most one shaded 1-band per n -band and there are no unshaded 1-bands in the top and bottom $(n-1)$ -bands. Secondly, the total number of 1-bands is $m'-2$ and there are $m-1$ shaded 1-bands, so there must be $m'-m-1$ unshaded 1-bands. Combining these two expressions gives (B.5b). To obtain (B.5a), we use the fact that only two types of n -bands occur: shaded n -bands and n -bands with exactly one unshaded 1-band. When counting all the 1-bands by looking at n -bands, we count every 1-band n times, except for the $n-1$ 1-bands at the top and bottom. Starting at the bottom, the first 1-band gets counted once, the second 1-band twice and so on for the first $n-1$ 1-bands. Similarly, if we start at the top and work our way down. This means that overall we are undercounting in the first 1-band, by $n-1$ 1-bands, and in the second 1-band by $n-2$ 1-bands and so on through to undercounting by 1 in the last 1-band. This happens at both the top and bottom. Hence, to count all 1-bands n times, we need the boundary (last) term in the following expression

$$n \times \#1\text{-bands} = ns_n + nt_n + 2 \sum_{i=1}^{n-1} i = ns_n + nt_n + n(n-1) \quad (\text{B.16})$$

Dividing both sides by n and using the fact that there are $m'-2$ 1-bands in total, gives (B.5a).

B.2 Proof that $\rho = r \bmod n$

For the counting of shaded n -bands with $\lambda < \pi/n$, we prove the result $\rho = r \bmod n$. For $n = 1$ the result is trivial, so we can assume that $n \geq 2$. Each n -band must be a shaded n -band or it contains precisely one unshaded 1-band. We proceed iteratively in steps:

1. Consider the lowest n -band and set $r = \rho = 1$ where r counts the shaded n -bands from the bottom and ρ labels the current position which is a candidate for the position of a shaded n -band. The lowest n -band must be a shaded n -band (labelled by $r = 1$) or only contain one unshaded 1-band at the top.
2. (i) If both the current bottom n -band and the current bottom $(n+1)$ -band are shaded, the current n -band is a ground state n -band labelled by the current value of r at a height given by the current value of ρ . Increment $r \mapsto r + 1$, $\rho \mapsto \rho + 1$ and remove the bottom 1-band. Since the top $n-1$ 1-bands in the removed n -band were shaded, the next n -band up must be a shaded n -band or only contain one unshaded 1-band at the top.
(ii) If the current bottom n -band is shaded and the current bottom $(n+1)$ -band is not shaded, the current n -band is a ground state n -band labelled by the current value of r at a height given by the current value of ρ . Increment $r \mapsto r + 1$, $\rho \mapsto \rho + n + 1$ and remove the bottom $(n+1)$ -band. There are no further shaded n -bands involving the 1-bands that are removed. Since the top 1-band removed is unshaded, the next n -band up must be a shaded n -band or only contain one unshaded 1-band at the top.
(iii) If the current bottom n -band contains an unshaded 1-band, it must occur at the top of this n -band. This is not a ground state n -band. Increment $r \mapsto r$, $\rho \mapsto \rho + n$ and remove the bottom n -band. There are no further shaded n -bands involving the 1-bands that are removed. The next n -band up must be a shaded n -band or only contain one unshaded 1-band at the top.
3. Iterate step 2 until the top of the $A_{m'-1}$ diagram is reached and all 1-bands have been removed.
At each step we see that $\rho = r \bmod n$.

C $n = 2, 3$ Face Weights

Expressions for the $n \times n$ fused RSOS face weights have been obtained in [21]. In this appendix, we list explicitly the 19 and 44 face weights for $n = 2$ and $n = 3$. The number of face weights for general $n = 1, 2, 3, \dots$ is given by the octahedral numbers [59]

$$\frac{1}{3}((n+1)^3 + n + 1) = 6, 19, 44, 85, 146, \dots \quad (\text{C.1})$$

Adjacent heights $a, b = 1, \dots, m' - 1$ satisfy

$$|a - b| = \begin{cases} 0, 2, 4, \dots, n, & n \text{ even} \\ 1, 3, 5, \dots, n, & n \text{ odd} \end{cases} \quad n + 2 \leq a + b \leq 2m' - n - 2 \quad (\text{C.2})$$

C.1 Explicit 2×2 fused face weights

The normalized 2×2 fused RSOS face weights are

$$W^{2,2} \left(\begin{array}{c|c} d & c \\ \hline a & b \end{array} \middle| u \right) = \frac{1}{\eta^{2,2}(u)} \begin{array}{|c|c|} \hline \begin{array}{c} u \\ \bullet \end{array} & \begin{array}{c} u + \lambda \\ \times \end{array} \\ \hline \begin{array}{c} u - \lambda \\ \bullet \end{array} & \begin{array}{c} u \\ \bullet \end{array} \\ \hline \end{array} \quad (\text{C.3})$$

The black dots indicate sums over all allowed heights at the site. The crosses indicate that the weight is independent of the allowed heights on these sites. The fused weights all have a common factor which

is removed

$$\eta^{2,2}(u) = s(2\lambda)s(u)s(u - \lambda) \quad (\text{C.4})$$

The explicit formulas for all 19 types of weights are

$$W^{2,2} \left(\begin{array}{cc|c} a \pm 2 & a & u \\ a & a \mp 2 & \end{array} \right) = \frac{s(u - 2\lambda)s(u - \lambda)}{s(2\lambda)} \quad (\text{C.5a})$$

$$W^{2,2} \left(\begin{array}{cc|c} a & a & u \\ a & a \pm 2 & \end{array} \right) = W^{2,2} \left(\begin{array}{cc|c} a \pm 2 & a & u \\ a & a & \end{array} \right) = -\frac{s(u - \lambda)s((a \pm 1)\lambda \mp u)}{s((a \pm 1)\lambda)} \quad (\text{C.5b})$$

$$W^{2,2} \left(\begin{array}{cc|c} a & a & u \\ a \pm 2 & a & \end{array} \right) = -\frac{s((a \mp 1)\lambda)s(u)s(a\lambda \pm u)}{s(2\lambda)s(a\lambda)s((a \pm 1)\lambda)} \quad (\text{C.5c})$$

$$W^{2,2} \left(\begin{array}{cc|c} a & a \pm 2 & u \\ a & a & \end{array} \right) = -\frac{s(2\lambda)s((a \pm 2)\lambda)s(u)s(a\lambda \pm u)}{s((a - 1)\lambda)s((a + 1)\lambda)} \quad (\text{C.5d})$$

$$W^{2,2} \left(\begin{array}{cc|c} a & a \mp 2 & u \\ a \pm 2 & a & \end{array} \right) = \frac{s((a \mp 2)\lambda)s((a \mp 1)\lambda)s(u)s(\lambda + u)}{s(2\lambda)s(a\lambda)s((a \pm 1)\lambda)} \quad (\text{C.5e})$$

$$W^{2,2} \left(\begin{array}{cc|c} a & a \pm 2 & u \\ a \pm 2 & a & \end{array} \right) = \frac{s(a\lambda \pm u)s((a \pm 1)\lambda \pm u)}{s(a\lambda)s((a \pm 1)\lambda)} \quad (\text{C.5f})$$

$$W^{2,2} \left(\begin{array}{cc|c} a & a & u \\ a & a & \end{array} \right) = \frac{s(a\lambda \pm u)s((a \pm 1)\lambda \mp u)}{s(a\lambda)s((a \pm 1)\lambda)} + \frac{s((a \pm 1)\lambda)s((a \mp 2\lambda))s(u)s(u - \lambda)}{s(2\lambda)s(a\lambda)s((a \mp 1)\lambda)} \quad (\text{C.5g})$$

$$W^{2,2} \left(\begin{array}{cc|c} a & a \pm 2 & u \\ a & a \pm 2 & \end{array} \right) = W^{2,2} \left(\begin{array}{cc|c} a \pm 2 & a \pm 2 & u \\ a & a & \end{array} \right) = \frac{s((a \pm 3)\lambda)s(u)s(u - \lambda)}{s(2\lambda)s((a \pm 1)\lambda)} \quad (\text{C.5h})$$

C.2 Explicit 3×3 fused face weights

The normalized 3×3 fused RSOS face weights are

$$W^{3,3} \left(\begin{array}{cc|c} d & c & u \\ a & b & \end{array} \right) = \frac{1}{\eta^{3,3}(u)} \quad (\text{C.6})$$

with normalization

$$\eta^{3,3}(u) = s(2\lambda)s(3\lambda)s(u - 2\lambda)s^2(u - \lambda)s^2(u)s(u + \lambda) \quad (\text{C.7})$$

$$W^{3,3} \left(\begin{array}{cc|c} a \pm 3 & a & u \\ a & a \pm 3 & \end{array} \right) = \frac{s((a \pm 1)\lambda \mp u)s((a \pm 2)\lambda \mp u)s((a \pm 3)\lambda \mp u)}{s((a \pm 1)\lambda)s((a \pm 2)\lambda)s((a \pm 3)\lambda)} \quad (\text{C.8a})$$

$$W^{3,3} \left(\begin{array}{cc|c} a \mp 3 & a & u \\ a & a \pm 3 & \end{array} \right) = \frac{s(\lambda - u)s(2\lambda - u)s(3\lambda - u)}{s(2\lambda)s(3\lambda)} \quad (\text{C.8b})$$

$$W^{3,3} \left(\begin{array}{cc|c} a \pm 1 & a & u \\ a & a \pm 3 & \end{array} \right) = W^{3,3} \left(\begin{array}{cc|c} a \pm 3 & a & u \\ a & a \pm 1 & \end{array} \right) = \frac{s(\lambda - u)s((a \pm 1)\lambda \mp u)s((a \pm 2)\lambda \mp u)}{s((a \pm 1)\lambda)s((a \pm 2)\lambda)} \quad (\text{C.8c})$$

$$W^{3,3} \left(\begin{array}{cc|c} a \mp 1 & a & u \\ a & a \pm 3 & \end{array} \right) = W^{3,3} \left(\begin{array}{cc|c} a \pm 3 & a & u \\ a & a \mp 1 & \end{array} \right) = \frac{s(\lambda - u)s(2\lambda - u)s((a \pm 1)\lambda \mp u)}{s(2\lambda)s((a \pm 1)\lambda)} \quad (\text{C.8d})$$

$$W^{3,3} \left(\begin{array}{c|c} a \pm 1 & a \\ a & a \pm 1 \end{array} \middle| u \right) = \frac{s((a \pm 1)\lambda \mp u)s((a \pm 1)\lambda \pm u)s((a \pm 2)\lambda \mp u)}{s((a \pm 1)\lambda)^2 s((a \pm 2)\lambda)} - \frac{s(2\lambda)s((a - 2)\lambda)s((a + 2)\lambda)s(\lambda - u)s(u)s((a \pm 1)\lambda \mp u)}{s(3\lambda)s((a \mp 1)\lambda)s((a \pm 1)\lambda)^2} \quad (\text{C.8e})$$

$$W^{3,3} \left(\begin{array}{c|c} a \mp 1 & a \\ a & a \pm 1 \end{array} \middle| u \right) = \frac{s(2\lambda)^2 s((a \mp 2)\lambda)s(\lambda - u)s(a\lambda \pm u)s((a \pm 1)\lambda \mp u)}{s(3\lambda)s((a \mp 1)\lambda)^2 s((a \pm 1)\lambda)} - \frac{s((a \mp 3)\lambda)s((a \pm 1)\lambda)s(2\lambda - u)s(\lambda - u)s(\lambda + u)}{s(2\lambda)s(3\lambda)s((a \mp 1)\lambda)^2} \quad (\text{C.8f})$$

$$W^{3,3} \left(\begin{array}{c|c} a \pm 3 & a \pm 6 \\ a & a \pm 3 \end{array} \middle| u \right) = -\frac{s((a \pm 4)\lambda)s((a \pm 5)\lambda)s((a \pm 6)\lambda)s(u)s(\lambda + u)s(2\lambda + u)}{s(2\lambda)s(3\lambda)s((a \pm 1)\lambda)s((a \pm 2)\lambda)s((a \pm 3)\lambda)} \quad (\text{C.8g})$$

$$W^{3,3} \left(\begin{array}{c|c} a \pm 3 & a \pm 4 \\ a & a \pm 3 \end{array} \middle| u \right) = \frac{s((a \pm 4)\lambda)s((a \pm 5)\lambda)s(u)s(\lambda + u)s((a \pm 3)\lambda \mp u)}{s(2\lambda)s(3\lambda)s((a \pm 1)\lambda)s((a \pm 2)\lambda)s((a \pm 3)\lambda)} \quad (\text{C.8h})$$

$$W^{3,3} \left(\begin{array}{c|c} a \pm 1 & a \pm 4 \\ a & a \pm 3 \end{array} \middle| u \right) = W^{3,3} \left(\begin{array}{c|c} a \pm 3 & a \pm 4 \\ a & a \pm 1 \end{array} \middle| u \right) = -\frac{s((a \pm 4)\lambda)s((a \pm 5)\lambda)s(u)s(u - \lambda)s(\lambda + u)}{s(2\lambda)s(3\lambda)s((a \pm 1)\lambda)s((a \pm 2)\lambda)} \quad (\text{C.8i})$$

$$W^{3,3} \left(\begin{array}{c|c} a \pm 3 & a \pm 2 \\ a & a \pm 3 \end{array} \middle| u \right) = -\frac{s((a \pm 4)\lambda)s(u)s((a \pm 2)\lambda \mp u)s((a \pm 3)\lambda \mp u)}{s(3\lambda)s((a \pm 1)\lambda)s((a \pm 2)\lambda)s((a \pm 3)\lambda)} \quad (\text{C.8j})$$

$$W^{3,3} \left(\begin{array}{c|c} a \pm 1 & a \pm 2 \\ a & a \pm 3 \end{array} \middle| u \right) = W^{3,3} \left(\begin{array}{c|c} a \pm 3 & a \pm 2 \\ a & a \pm 1 \end{array} \middle| u \right) = \frac{s((a \pm 4)\lambda)s(u)s(u - \lambda)s((a \pm 2)\lambda \mp u)}{s(3\lambda)s((a \pm 1)\lambda)s((a \pm 2)\lambda)} \quad (\text{C.8k})$$

$$W^{3,3} \left(\begin{array}{c|c} a \mp 1 & a \pm 2 \\ a & a \pm 3 \end{array} \middle| u \right) = W^{3,3} \left(\begin{array}{c|c} a \pm 3 & a \pm 2 \\ a & a \mp 1 \end{array} \middle| u \right) = -\frac{s((a \pm 4)\lambda)s(2\lambda - u)s(\lambda - u)s(u)}{s(2\lambda)s(3\lambda)s((a \pm 1)\lambda)} \quad (\text{C.8l})$$

$$W^{3,3} \left(\begin{array}{c|c} a \pm 1 & a \pm 4 \\ a & a \pm 1 \end{array} \middle| u \right) = \frac{s(3\lambda)s((a \pm 3)\lambda)(s(a \pm 4)\lambda)s(u)s(u + \lambda)s((a \pm 1)\lambda \pm u)}{s(2\lambda)s((a - 1)\lambda)s((a + 1)\lambda)s((a \pm 2)\lambda)} \quad (\text{C.8m})$$

$$W^{3,3} \left(\begin{array}{c|c} a \pm 1 & a \pm 2 \\ a & a \pm 1 \end{array} \middle| u \right) = -\frac{s(a\lambda)s((a \pm 3)\lambda)s((a \pm 4)\lambda)s(u)^2 s(u - \lambda)}{s(2\lambda)s(3\lambda)s((a \pm 1)\lambda)^2 s((a \pm 2)\lambda)} - \frac{s((a \pm 3)\lambda)s(u)s(a\lambda \pm u)s((a \pm 1)\lambda \mp u)}{s((a \mp 1)\lambda)s((a \pm 1)\lambda)^2} \quad (\text{C.8n})$$

$$W^{3,3} \left(\begin{array}{c|c} a \mp 1 & a \pm 2 \\ a & a \pm 1 \end{array} \middle| u \right) = W^{3,3} \left(\begin{array}{c|c} a \pm 1 & a \pm 2 \\ a & a \mp 1 \end{array} \middle| u \right) = \frac{s((a \pm 3)\lambda)s(u)s(u - \lambda)s(a\lambda \pm u)}{s((a - 1)\lambda)s((a + 1)\lambda)} \quad (\text{C.8o})$$

$$W^{3,3} \left(\begin{array}{c|c} a \pm 1 & a \mp 2 \\ a & a \pm 1 \end{array} \middle| u \right) = -\frac{s(3\lambda)s((a \mp 2)\lambda)s(u)s(a\lambda \mp u)s((a \pm 1)\lambda \mp u)}{s((a - 1)\lambda)s((a + 1)\lambda)s((a \pm 2)\lambda)} \quad (\text{C.8p})$$

D $n = 2, 3$ Diagonal Conjugate Modulus Face Weights

In this appendix, we list the diagonal conjugate modulus face weights for $n = 2$ and $n = 3$.

D.1 Explicit 2×2 conjugate modulus face weights

The explicit 2×2 diagonal conjugate modulus face weights are

$$W^{2,2} \left(\begin{array}{c|c} a \pm 2 & a \\ a & a \mp 2 \end{array} \right) = \frac{g_a^2}{g_{a-2}g_{a+2}} w \frac{E(x^2 w^{-1})E(xw^{-1})}{E(x^2)E(x)} \quad (\text{D.1a})$$

$$W^{2,2} \left(\begin{array}{c|c} a & a \\ a & a \pm 2 \end{array} \right) = W^{2,2} \left(\begin{array}{c|c} a \pm 2 & a \\ a & a \end{array} \right) = \frac{g_a}{g_{a \pm 2}} \frac{E(xw^{-1})E(x^{a \pm 1} w^{\mp 1})}{E(x)E(x^{a \pm 1})} \quad (\text{D.1b})$$

$$W^{2,2} \left(\begin{array}{c|c} a & a \pm 2 \\ a \pm 2 & a \end{array} \right) = \frac{g_{a \pm 2}^2}{g_a^2} \frac{E(x^a w^{\pm 1})E(x^{a \pm 1} w^{\pm 1})}{E(x^a)E(x^{a \pm 1})} \quad (\text{D.1c})$$

$$W^{2,2} \begin{pmatrix} a & a \\ a & a \end{pmatrix} = wx \frac{E(x^{a-1})E(x^{a+2})E(w^{-1})E(xw^{-1})}{E(x)E(x^2)E(x^a)E(x^{a+1})} + \frac{E(x^{a-1}w)E(x^a w^{-1})}{E(x^{a-1})E(x^a)} \quad (\text{D.1d})$$

D.2 Explicit 3×3 conjugate modulus face weights

The explicit 3×3 diagonal conjugate modulus face weights are

$$W^{3,3} \begin{pmatrix} a \pm 3 & a \\ a & a \pm 3 \end{pmatrix} \Big| u = \frac{g_a^2}{g_{a \pm 3}^2} \frac{E(x^{a \pm 1} w^{\mp 1}) E(x^{a \pm 2} w^{\mp 1}) E(x^{a \pm 3} w^{\mp 1})}{E(x^{a \pm 1}) E(x^{a \pm 2}) E(x^{a \pm 3})} \quad (\text{D.2a})$$

$$W^{3,3} \begin{pmatrix} a \pm 3 & a \\ a & a \pm 1 \end{pmatrix} \Big| u = W^{3,3} \begin{pmatrix} a \pm 1 & a \\ a & a \pm 3 \end{pmatrix} \Big| u = \frac{g_a^2}{g_{a \pm 1} g_{a \pm 3}} \frac{w^{1/2} E(xw^{-1}) E(x^{a \pm 1} w^{\mp 1}) E(x^{a \pm 2} w^{-1})}{E(x) E(x^{a \pm 1}) E(x^{a \pm 2})} \quad (\text{D.2b})$$

$$W^{3,3} \begin{pmatrix} a \pm 3 & a \\ a & a \mp 1 \end{pmatrix} \Big| u = W^{3,3} \begin{pmatrix} a \mp 1 & a \\ a & a \pm 3 \end{pmatrix} \Big| u = \frac{g_a^2}{g_{a \mp 1} g_{a \pm 3}} \frac{w E(xw^{-1}) E(x^2 w^{-1}) E(x^{a \pm 1} w^{\mp 1})}{E(x) E(x^2) E(x^{a \pm 1})} \quad (\text{D.2c})$$

$$W^{3,3} \begin{pmatrix} a \pm 3 & a \\ a & a \mp 3 \end{pmatrix} \Big| u = \frac{g_a^2}{g_{a \pm 3} g_{a \mp 3}} \frac{w^{3/2} E(xw^{-1}) E(x^2 w^{-1}) E(x^3 w^{-1})}{E(x) E(x^2) E(x^3)} \quad (\text{D.2d})$$

$$W^{3,3} \begin{pmatrix} a \pm 1 & a \\ a & a \pm 1 \end{pmatrix} \Big| u = \frac{g_a^2}{g_{a \pm 1}^2} \left(\frac{E(x^{a \pm 1} w^{\mp 1}) E(x^{a \pm 1} w^{\pm 1}) E(x^{a \pm 2} w^{\mp 1})}{E(x^{a \pm 1})^2 E(x^{a \pm 2})} \right. \\ \left. - \frac{x E(x^2) E(x^{a+2}) E(x^{a-2}) E(w) E(xw^{-1}) E(x^{a \pm 1} w^{\mp 1})}{E(x)^2 E(x^3) E(x^{a \mp 1}) E(x^{a \pm 1})^2} \right) \quad (\text{D.2e})$$

$$W^{3,3} \begin{pmatrix} a \pm 1 & a \\ a & a \mp 1 \end{pmatrix} \Big| u = \frac{g_a^2}{g_{a \pm 1} g_{a \mp 1}} \left(\frac{w^{1/2} E(x^2)^2 E(x^{a \pm 2}) E(xw^{-1}) E(x^{a \mp 1} w^{\pm 1}) E(x^a w^{\mp 1})}{E(x)^2 E(x^3) E(x^{a \mp 1}) E(x^{a \pm 1})^2} \right. \\ \left. - \frac{w^{1/2} x E(x^{a \mp 1}) E(x^{a \pm 3}) E(xw^{-1}) E(xw) E(x^2 w^{-1})}{E(x) E(x^2) E(x^3) E(x^{a \pm 1})^2} \right) \quad (\text{D.2f})$$

References

- [1] H. van Beijeren, *Exactly solvable model for the roughening transition of a crystal surface*, Phys. Rev. Lett. **38** (1977) 993–996.
- [2] H.J.F. Knops, *Exact relation between the solid-on-solid model and the XY model*, Phys. Rev. Lett. **39** (1977) 766–769.
- [3] S.T. Chui, J.D. Weeks, *Pinning and roughening of one-dimensional models of interfaces and steps*, Phys. Rev. **B23** (1981) 2438–2441.
- [4] J.M. Luck, *Finite-size lattice method and the roughening transition*, J. Physique Lett. **42** (1981) L275–277.
- [5] G.E. Andrews, R.J. Baxter and P.J. Forrester, *Eight-vertex SOS model and generalised Rogers-Ramanujan-type identities*, J. Stat. Phys. **35** (1984) 193–266.
- [6] P.J. Forrester and R.J. Baxter, *Further exact solutions of the eight-vertex SOS model and generalizations of the Rogers-Ramanujan identities*, J. Stat. Phys. **38** (1985) 435–472.

- [7] R.J. Baxter, *Exactly Solved Models in Statistical Mechanics*, London: Academic Press, 1982.
- [8] D.A. Huse, *Exact exponents for infinitely many new multicritical points*, Phys. Rev. **B30** (1984) 3908–3915.
- [9] P. Di Francesco, P. Mathieu and D. Sénéchal, *Conformal Field Theory*, New York: Springer, 1997.
- [10] D. Friedan, Z. Qiu and S. Shenker, *Conformal invariance, unitarity and critical exponents in two dimensions*, Phys. Rev. Lett. **52** (1984) 1575.
- [11] C. Itzykson, H. Saleur and J.-B. Zuber, *Conformal invariance of nonunitary 2d-models*, Europhys. Lett. **2** (1986) 91–96.
- [12] H. Riggs, *Solvable lattice models with minimal and nonunitary critical behaviour in two dimensions*, Nucl. Phys. **B326** (1989) 673–688.
- [13] T. Nakanishi, *Non-unitary minimal models and RSOS models*, Nucl. Phys. **B334** (1990) 745–766.
- [14] O. Foda and T.A. Welsh, *On the combinatorics of Forrester-Baxter models*, Physical Combinatorics (Kyoto, 1999), Progress in Mathematics **191** (2000) 49–103, Birkhauser, Boston, MA.
- [15] A.A. Belavin, A.M. Polyakov and A.B. Zamolodchikov, *Infinite conformal symmetry in two-dimensional quantum field theory*, Nucl. Phys. **B241** (1984) 333–380; *Infinite conformal symmetry of critical fluctuations in two dimensions*, J. Stat. Phys. **34** (1984) 763–774.
- [16] P. Goddard, A. Kent, D. Olive, *Virasoro algebras and coset space models*, Phys. Lett. **B152** (1985) 88–92.
- [17] P. Goddard, A. Kent, D. Olive, *Unitary representations of the Virasoro and super-Virasoro algebras*, Commun. Math. Phys. **103** (1986) 105–119.
- [18] P.P. Kulish, N.Y. Reshetikhin, E.K. Sklyanin, *Yang-Baxter equation and representation theory: I*, Lett. Math. Phys. **5** (1981) 393–403.
- [19] G.E. Andrews, R.J. Baxter, *Lattice gas generalization of the hard hexagon model. I. Star-triangle relation and local densities*, J. Stat. Phys. **44** (1986) 249–271; *Lattice gas generalization of the hard hexagon model. II. The local densities as elliptic functions*, J. Stat. Phys. **44** (1986) 713–728; *Lattice gas generalization of the hard hexagon model. III. q-trinomial coefficients*, J. Stat. Phys. **47** (1987) 297–330;
- [20] E. Date, M. Jimbo, T. Miwa and M. Okado, *Fusion of the eight vertex SOS model*, Lett. Math. Phys. **12** (1986) 209–215; *Automorphic properties of local height probabilities for integrable solid-on-solid models*, Phys. Rev. **B35** (1987) 2105–2107.
- [21] E. Date, M. Jimbo, A. Kuniba, T. Miwa and M. Okado, *Exactly solvable SOS models: I. Local height probabilities and theta function identities*, Nucl. Phys. B **290** [FS20] (1987) 231–273; *Exactly solvable SOS models: II. Proof of star-triangle relation and combinatorial identities*, Adv. Stud. Pure Math. **16** (1988) 17–122.
- [22] V.G. Kac, D.H. Peterson, *Infinite-dimensional Lie algebras, theta functions and modular forms*, Adv. in Math. **53** (1984) 125–264.
- [23] D. Kastor, E. Martinec and Z. Qiu, *Current algebra and conformal discrete series*, Phys. Lett. **B200** (1988) 434.
- [24] J. Bagger, D. Nemeschansky, S. Yankielowicz, *Virasoro algebras with central charge $c > 1$* , Phys. Rev. Lett. **60** (1988) 389.

- [25] F. Ravanini, *An extended class of new conformal field theories with extended algebras*, Mod. Phys. Lett. **A3** (1988) 397.
- [26] C. Ahn, S.-W. Chung, S.-H. Tye, *New parafermion, $SU(2)$ coset and $N = 2$ superconformal field theories*, Nucl. Phys. **B365** (1991) 191–240.
- [27] A. Berkovich, B.M. McCoy, A. Schilling, S.O. Warnaar, *Bailey flows and Bose-Fermi identities for the conformal coset models $(A_1^{(1)})_N \times (A_1^{(1)})_{N'}/(A_1^{(1)})_{N+N'}$* , Nucl. Phys. **B499** (1997) 621–649.
- [28] V.V. Bazhanov, N.Y. Reshetikhin, *Critical RSOS models and conformal field theory*, Int. J. Mod. Phys. A **04** (1989) 115.
- [29] A. Klümper and P.A. Pearce, *Conformal weights of RSOS lattice models and their fusion hierarchies*, Physica **A183** (1992) 304–350.
- [30] A. Schilling, *Multinomials and polynomial bosonic forms for the branching functions of the $\hat{su}(2)_M \times \hat{su}(2)_N/\hat{su}(2)_{M+N}$ conformal coset models*, Nucl. Phys. **B467** (1996) 247–271.
- [31] R.J. Baxter, *Corner transfer matrices of the eight-vertex model I. Low temperature expansions and conjectured properties*, J. Stat. Phys. **15** (1976) 485–503; *Corner transfer matrices of the eight-vertex model II. The Ising model case*, J. Stat. Phys. **17** (1977) 1–14.
- [32] M. Jimbo, T. Miwa, *Algebraic analysis of solvable lattice models*, CBMS Regional Conference Series in Mathematics, AMS **85** (1993).
- [33] P.A. Pearce, B. Nienhuis, *Scaling limit of RSOS lattice models and TBA equations*, Nucl. Phys. **B519** (1998) 579–596.
- [34] Mathematica 8, Wolfram Research, Inc., Champaign IL (2010).
- [35] S.O. Warnaar, *The Andrews-Gordon identities and q -multinomial coefficients*, Commun. Math. Phys. **184** (1997) 203–232.
- [36] D. Bianchini, E. Ercolessi, P.A. Pearce, F. Ravanini, *RSOS quantum chains associated with off-critical minimal models and \mathbb{Z}_n parafermions*, J. Stat. Mech. (2015) P03010.
- [37] C.-N. Yang, T.D. Lee, *Statistical theory of equations of state and phase transitions. 1. Theory of condensation*, Phys. Rev. **87** (1952) 404; T.D. Lee, C.-N. Yang, *Statistical theory of equations of state and phase transitions. 2. Lattice gas and Ising model*, Phys. Rev. **87** (1952) 410.
- [38] M.E. Fisher, *Yang-Lee edge singularity and ϕ^3 field theory*, Phys. Rev. Lett. **40** (1978) 1610.
- [39] J.L. Cardy, *Conformal invariance and the Yang-Lee edge singularity in two-dimensions*, Phys. Rev. Lett. **54** (1985) 1354.
- [40] J.L. Cardy, G. Mussardo, *S matrix of the Yang-Lee edge singularity in two-dimensions*, Phys. Lett. **B225** (1989) 275–278.
- [41] A.B. Zamolodchikov, *Thermodynamic Bethe Ansatz in relativistic models. Scaling three state Potts and Lee-Yang models*, Nucl. Phys. **B342** (1990) 695–720.
- [42] Z. Bajnok, O. el Deeb, P.A. Pearce, *Finite-volume spectra of the Lee-Yang model*, J. High Energy Physics JHEP04 (2015) 073.
- [43] O. el Deeb, *On the critical boundary RSOS $\mathcal{M}(3, 5)$ model*, [arXiv:1512.02185](https://arxiv.org/abs/1512.02185) (2015).

- [44] S.H. Simon, E.H. Rezayi, N.R. Cooper, I. Berdnikov, *Construction of a paired wave function for spinless electrons at filling fraction $\nu = 2/5$* , Phys. Rev. **B75** (2007) 075317.
- [45] D. Bianchini, F. Ravanini, *Entanglement entropy from corner transfer matrix in Forrester Baxter non-unitary RSOS models*, [arXiv:1509.04601](https://arxiv.org/abs/1509.04601) (2015).
- [46] V. Gurarie, *Logarithmic operators in conformal field theory*, Nucl. Phys. **B410** (1993) 535–549.
- [47] A. Gainutdinov, D. Ridout, I. Runkel (Guest Editors), *Special issue on logarithmic conformal field theory*, J. Phys. A: Math. Theor. **46** (2013) Number 49.
- [48] P.A. Pearce, J. Rasmussen, J.-B. Zuber, *Logarithmic minimal models*, J. Stat. Mech. (2006) P11017.
- [49] P.A. Pearce, J. Rasmussen, *Coset construction of logarithmic minimal models: branching rules and branching functions*, J. Phys. A **46** (2013) 355402 (14pp).
- [50] P.A. Pearce, J. Rasmussen, E. Tartaglia, *Logarithmic superconformal minimal models*, J. Stat. Mech. (2014) P05001.
- [51] J. Rasmussen, *Logarithmic limits of minimal models*, Nucl. Phys. **B701** (2004) 516–528; *Jordan cells in logarithmic limits of conformal field theory*, Int. J. Mod. Phys. **A22** (2007) 67–82.
- [52] M. Jimbo, T. Miwa, *Irreducible decomposition of fundamental modules for $A_\ell^{(1)}$ and $C_\ell^{(1)}$ and Hecke modular forms*, Adv. Stud. Pure Math. **4** (1984) 97–119.
- [53] D. Gepner, Z. Qiu, *Modular invariant partition functions for parafermionic field theories*, Nucl. Phys. **B285** (1987) 423–453.
- [54] J. Distler, Z. Qiu, *BRS cohomology and a Feigin-Fuchs representation of Kac-Moody and parafermionic theories*, Nucl. Phys. **B336** (1990) 533–546.
- [55] K. Huitu, D. Nemeschansky, S. Yankielowicz, *$N = 2$ supersymmetry, coset models and characters*, Phys. Lett. **B246** (1990) 105–113.
- [56] I.S. Gradshteyn and I.M. Ryzhik, *Tables of Integrals, Series and Products*, New York; Sydney: Academic Press, 1980.
- [57] A.B. Zamolodchikov, *Higher-order integrals of motion in two-dimensional models of field theory with a broken conformal symmetry*, JETP Lett. **46** (1987) 160; *Integrals of motion in scaling 3-state Potts model field theory*, Int. J. Mod. Phys. **A3** (1988) 743; *Integrable field theory from conformal field theory*, Adv. Stud. Pure Math. **19** (1989) 641.
- [58] A. Schilling, S.O. Warnaar, *Supernomial coefficients, polynomial identities and q -series*, Ramanujan Journal **2** (1998) 459–494; *Conjugate Bailey pairs. From configuration sums and fractional-level string functions to Bailey’s lemma*, in S. Berman et al. eds., Recent Developments in Infinite-Dimensional Lie Algebras and Conformal Field Theory, Contemp. Math. 297, (AMS, Providence, 2002), 227–255.
- [59] N.J.A. Sloane, *The On-Line Encyclopedia of Integer Sequences*, published electronically at <http://oeis.org>, Sequence A005900 (octahedral numbers).